Sensitivity analysis methods for uncertainty budgeting in system design

Sensitivity Analysis Methods for Uncertainty Budgeting in System Design

Max M. J. Opgenoord* and Karen E. Willcox†

Massachusetts Institute of Technology, Cambridge, MA, 02139

Quantification and management of uncertainty are critical in the design of engineering systems, especially in the early stages of conceptual design. This paper presents an approach to defining budgets on the acceptable levels of uncertainty in design quantities of interest, such as the allowable risk in not meeting a critical design constraint and the allowable deviation in a system performance metric. A sensitivity-based method analyzes the effects of design decisions on satisfying those budgets, and a multi-objective optimization formulation permits the designer to explore the tradespace of uncertainty reduction activities while also accounting for a cost budget. For models that are computationally costly to evaluate, a surrogate modeling approach based on high dimensional model representation (HDMR) achieves efficient computation of the sensitivities. An example problem in aircraft conceptual design illustrates the approach.

Nomenclature

C	Cost of changing the distributions of the input variables	$f_Y(r)$	Value of the probability density function of y at $y = r$
C_L	Cruise aircraft lift coefficient	g	Engineering system representation, prescribing the relation between the input variables and the QoI
C_b	Budget on the cost of changes in the input distributions	g_0, g_i, g_{ij}, ...	Component functions of HDMR surrogate
$\mathcal{F}$	Objective function for optimization problem	n	Number of input variables
$\mathcal{G}$	Nonlinear constraint for optimization problem	$\hat{p}$	Risk of QoI y exceeding the value r
K^n	Input space mapped to the unit hypercube	s_{fus}	Maximum allowable fuselage shell bending stress
$MTOW$	Maximum Takeoff Weight	s_{wt}	Maximum allowable wing and tail spar cap stress
N	Number of samples	$\mathbf{x}$, x_i, x_j	Input variables
OPR	Overall pressure ratio	y	Quantity of interest (QoI)
P	Risk of QoI exceeding r	*Symbols*	
P_0	Risk of QoI exceeding r for nominal input variable distributions	α, β, γ	Weighting parameters for the objective function
P_b	Budget on the risk of the QoI	α_r^i	Weighting coefficient for first-order component functions
P'	Updated risk for changes in the distributions of the input variables	β_{pq}^{ij}	Weighting coefficient for second-order component functions
S_i, S_{ij}, ...	Sensitivity indices	$\boldsymbol{\mu}$	Vector containing the mean of each input variable
T_{metal}	Turbine metal temperature	μ_Y	Mean of QoI
$(T_{t4})_{\text{CR}}$	Turbine inlet total temperature for cruise	$\boldsymbol{\sigma}$	Vector containing the standard deviation of each input variable
V_i, V_{ij}, ...	Variance of component functions of HDMR		
f	Probability density function		

*Graduate student, Department of Aeronautics and Astronautics, mopg@mit.edu, Student Member AIAA

†Professor of Aeronautics and Astronautics, kwillcox@mit.edu, Associate Fellow AIAA

σ_Y	Standard deviation of QoI	φ_i	Basis functions
$\sigma_{Y,b}$	Budget on the standard deviation of the QoI	ξ	Running parameter for basis functions

I. Introduction

THIS paper presents a sensitivity-based methodology to support decision-making in the design of multidisciplinary engineering systems, with a focus on the challenge of quantifying and managing uncertainty. We consider the early stages of the design phase, where quantification of uncertainty permits designers to identify critical areas of design risk and to allocate resources accordingly.Uncertainties abound in engineering design and decision: technical uncertainties due to novel configurations and new technologies, programmatic uncertainties in cost and schedule, design requirements and/or operating conditions that may evolve over time, and uncertainties introduced due to the use of simplified models. These uncertainties pose a serious risk to the critical decisions made in engineering design, especially when considering novel systems for which experience and historical data are lacking. Despite a growing recognition of the importance of accounting for uncertainties, systematic methods to quantify and manage uncertainty remain a significant challenge, especially for systems that comprise many interacting subcomponents and/or disciplines.

Past work has addressed the challenge of forward propagation of uncertainty: Given uncertain parameters and uncertain system inputs, what is the corresponding uncertainty in the outcome? Uncertain outcomes are typically characterized by uncertainty associated with the design quantities of interest (QoI).[1,2,3] The literature categorizes uncertainty as epistemic, owing to insufficient or imperfect knowledge, or aleatory, which arises from natural randomness and is therefore irreducible.[2,4,5,6] Other work has distinguished among several types of uncertainty, including the many sources associated with the use of computer-based simulation models in system design.[7] In this paper, we use probabilistic models to represent uncertainty in design parameters and QoI.[2,8,9] Other ways of characterizing uncertainty include using a probability box to capture the imprecision in the available uncertainty information.[10] Regardless of the method chosen to represent uncertainty, forward propagation of uncertainty typically involves repeated model evaluations to conduct the needed sampling; thus, a great deal of recent work has focused on methods to reduce computational expense, including the use of less-expensive surrogate models to approximate system response.[11,12,13,14,15,16]

Sensitivity analysis targets the inverse question: What are the uncertain parameters and inputs that contribute the most to output variability, and how would reducing uncertainty in these parameters lead to reduction in output uncertainty? In the context of engineering system design, sensitivity analysis permits better understanding of the effects of uncertainty in order to make well-informed decisions aimed at uncertainty reduction.[8,17] Existing sensitivity analysis approaches typically use variance as a measure of uncertainty. The process of apportioning output variance across model factors in a global sensitivity analysis can be carried out by both a Fourier Amplitude Sensitivity Test (FAST) method, and the Sobol' method.[18,19,20,21,22] The FAST method is based on Fourier transforms, while the Sobol' method utilizes Monte Carlo simulation. In addition to variance-based sensitivity analysis, work has also been done in the development of methods for global and regional sensitivity analysis using information entropy as a measure of uncertainty. One such method uses the Kullback-Leibler (K-L) divergence, or relative entropy, to quantify the distance between two probability distributions.[23] These distributions correspond to estimates of the QoI before and after some model parameter has been fixed at a particular value (e.g., its mean value). The K-L divergence between the two distributions then serves to quantify the impact of the factor that has been fixed: the larger the value of the K-L divergence, the more substantial the contribution of that parameter to uncertainty in the QoI.

In addressing design under uncertainty, robustness—which according to Knoll and Vogel is "the property of systems that enables them to survive unforeseen or unusual circumstances"[24]—and reliability—which describes a system's "probability of success in satisfying some performance criterion"[1]—are typically treated separately. The origins of robust design stem back to the pioneering work of Taguchi, with the aim of reducing the sensitivity of products and processes to various noise factors, such as manufacturing variability, environmental conditions, and degradation over time.[25,26,27] In Ref. 28, an integrated framework for optimization under uncertainty is developed that accounts for both design objective robustness and probabilistic design constraints.

This paper develops a broadly applicable sensitivity-based methodology that, given a model of the sources of uncertainty, provides systematic guidance to a decision-maker in identifying and selecting uncertainty reduction options and design choices. Our goal is to allocate the resources of cost, schedule and risk,

while also identifying opportunities to tailor the design so as to minimize uncertainty in key areas while retaining flexibility in others. Underlying our proposed approach is the view that uncertainty is a currency: a designer can tolerate a particular level of uncertainty, typically characterized by specified acceptable levels (i.e., budgets) of risk, reliability and/or robustness. The key challenge then becomes how to "spend" the uncertainty—where to focus uncertainty reduction efforts so as not to waste valuable resources reducing uncertainty in parameters that contribute little to output uncertainty, but instead to target the most sensitive parameters and manage resources in a systematic way. This modeling of the design process is consistent with decomposition-based formulations of the design problem, such as analytical target cascading (ATC), where the system is modeled using hierarchical levels and design targets are cascaded from upper levels to lower levels.[29,30,31] Similar ideas are explored in Chen et al., who propose a method that reverses the computational flow in a design code.[32] That work builds on the univariate reduced quadrature method of Padulo et al.,[33] which represents the QoI standard deviation as a function of the first four moments of a univariate input distribution.

Our work builds on the mathematical framework of Ref. 34, which views the system design problem as a stochastic estimation process as shown in Figure 1. The term "stochastic estimation process" is used to convey the idea that the design process can be modeled as an iterative process of resolving uncertainty. That is, at any point in time the design is represented through a set of state variables, each with an associated uncertainty. Design effort results in the generation of new information ("measurements"), which can be used to update the uncertain design state. This process continues until the uncertainty is resolved to acceptable levels. In this paper, we advance that work by formalizing the idea of uncertainty budgeting. In particular, we formulate and solve a multi-objective optimization problem that seeks optimal strategies to manage the uncertainty and design risk. A second contribution of the paper is to introduce a tailored surrogate modeling approach that permits analysis of complex system models. The remainder of the paper is organized as follows. Section II provides a description of the problem formulation and background on the sensitivity analysis methods. Section III describes the uncertainty budgeting methodology and formulates the resource allocation optimization problem. Section IV presents a surrogate modeling approach that can be used to reduce the computational expense of solving the uncertainty budgeting optimization problem. Section V demonstrates the approach by presenting illustrative examples in conceptual aircraft design focusing on propulsion uncertainty and uncertainty coming from multiple disciplines. Finally, Section VI concludes the paper.

II. Problem Formulation and Background

This section defines the problem formulation in Section II.A, and introduces background on high dimensional model representation (HDMR) and analysis of variance (ANOVA) in Section II.B.

II.A. Problem formulation

In the initial stages of designing a complex system, the key inputs for that design are still uncertain. In aircraft design, for instance, engine technology has a major influence on the design, but may not be fixed at the start of the design phase because of possible future advances.[36] However, the designers still have requirements for the system, and the risk of not meeting those requirements must be quantified and mitigated. Furthermore, key QoI describing the performance and cost of the design are also uncertain during early design stages. This uncertainty must be managed to acceptable levels as the design process evolves. In this work, we formalize the view that uncertainty is a currency: a designer can tolerate a particular level of uncertainty; the decision then becomes how to "spend" the uncertainty. To formulate this mathematically, we define *cost budgets* and *uncertainty budgets*. The uncertainty budget allocates quantitative limits on the acceptable risk in not meeting design requirements and on the acceptable variability in the design QoI (i.e., it specifies the desired reliability and robustness of the design). The cost budget allocates quantitative limits on the resources that can be expended on uncertainty reduction (e.g., money, time, computational resources).

We consider a general system, represented as

$$y = g(\mathbf{x}),$$

where y is the system QoI, $\mathbf{x}$ are the system input variables, and g is the mapping from input $\mathbf{x}$ to QoI y. Throughout this paper this system mapping is considered as a general black box—it could be, for example,

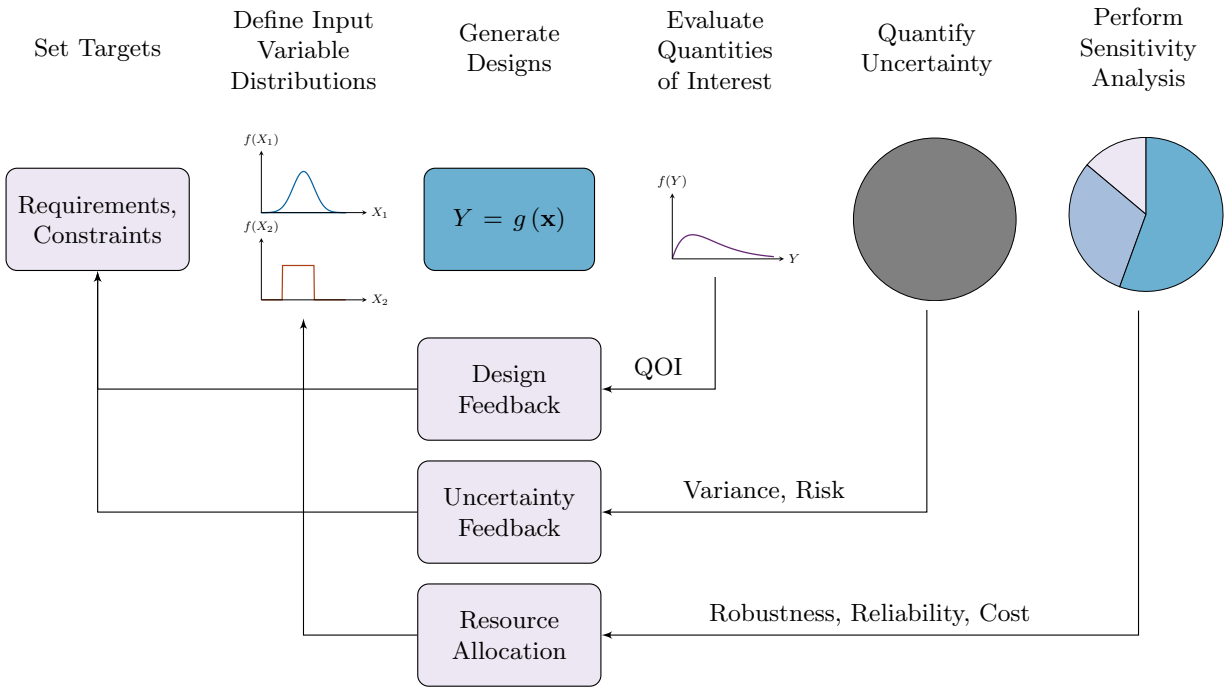

Figure 1. Modeling the system design as a stochastic estimation process with feedback. Figure adapted from Ref. 35.

a computational model or an experiment; however, it is assumed that there is freedom in choosing the input values (i.e., the function $g(\mathbf{x})$ can be evaluated for input $\mathbf{x}$). In the following we develop the methodology for a single scalar QoI, although the approach is straightforward to apply to the case of multiple QoI.

We represent the uncertainty in the input variables probabilistically, that is, we consider $\mathbf{x}$ to be a random variable and we describe each component of $\mathbf{x}$ using a probability density function (PDF). The PDFs for each input variable are specified by the designer and could be determined from historical data or expert opinion. In current engineering practices, such PDFs are typically not readily available and this is often put forward as a barrier against using probabilistic methods. In some cases, sufficient information and data will be available to infer a reasonable PDF—for example, when considering uncertainty associated with an advanced technology, one can often draw on experimental results that provide informed choices of parameter ranges and probable values. However, in many cases, engineering judgement will be required to define suitable PDFs for the input parameters. While this is certainly an important challenge that must be addressed, current design practices simply ignore uncertainty, or they account coarsely for it by using safety factors on the resulting design choices.[a]

The uncertainty in inputs induces uncertainty in the output QoI; thus, y is also modeled as a random variable. The PDF of y is estimated using Monte Carlo simulation to propagate uncertainty through the system. We then set budgets on allowable cost and uncertainty. In this work we consider a budget on the allowable standard deviation of the QoI, a budget on the allowable probability of not meeting design requirements, and a budget on the allowable cost of the changes in the input variables. Every design change has an associated cost—whether it be a cost associated with a change in the mean values of the input variables, or a cost associated with a reduction in input uncertainty. The problem therefore becomes a constrained optimization problem to find the best resource allocation strategy that satisfies both cost and uncertainty budgets. This is described mathematically in Section III. Our approach to formulating and solving this problem uses a global sensitivity analysis (GSA), built on the theory of high dimensional model representation (HDMR). The next subsection gives background on HDMR and GSA.

[a]As Richard Feynman eloquently puts it: "I can live with doubt and uncertainty and not knowing. I think it is much more interesting to live not knowing than to have answers that might be wrong. If we will only allow that, as we progress, we remain unsure, we will leave opportunities for alternatives."

II.B. High Dimensional Model Representation (HDMR) and Global Sensitivity Analysis (GSA)

HDMR is an analysis tool used in representing the relationship between inputs and outputs in a general model.[37,38,39] In this method, the function $g(\mathbf{x})$ is expanded into independent component subfunctions in terms of the input variables,

$$g(\mathbf{x}) = g_0 + \sum_{i=1}^{n} g_i(x_i) + \sum_{1\le i<j\le n} g_{ij}(x_i, x_j) + \ldots + \sum_{1\le i_1<\ldots<i_l\le n} g_{i_1 i_2 \ldots i_l}(x_{i_1}, x_{i_2}, \ldots, x_{i_l}) + \ldots + g_{12\ldots n}(x_1, x_2, \ldots, x_n). \quad (1)$$

Here, g_0 represents the mean response of $g(\mathbf{x})$ over the input space, while the component subfunction $g_i(x_i)$ captures the contribution of the ith input variable alone. We use the notation x_i to denote the ith input variable and we consider the case of n input variables, $\mathbf{x} = [x_1, \ldots, x_n]^\top$. The component subfunction $g_{ij}(x_i, x_j)$ represents the correlated contribution of the ith and jth input variable to $g(\mathbf{x})$, and so on.

The decomposition as written in Eq. (1) is not unique.[4] It can however be uniquely defined by imposing the vanishing condition,[40,41,42] which states that the integral of an HDMR component function with respect to any of its own variables is zero:[43]

$$\int_0^1 f_s(x_s)\, g_{i_1 i_2 \ldots i_k}(x_{i_1}, x_{i_2}, \ldots, x_{i_k})\, \mathrm{d}x_s = 0 \quad \forall s \in \{i_1, i_2, \ldots, i_k\}, \quad (2)$$

where $f_s(x_s)$ is the probability density function of the sth input variable. Note that for ease of presentation and without loss of generality, the variables x_i have been rescaled by a suitable transformation such that $0 \le x_i \le 1\ \forall i$. The HDMR representation with constraint (2) is called the ANOVA-HDMR; as described in the following, the resulting functional decomposition of $g(\mathbf{x})$ provides a quantitative basis on which to assess how the various inputs contribute to QoI uncertainty.[44,45]

Because of the orthogonality constraints in Eq. (2), the variance of the QoI can be expressed as

$$V(y) = \sum_i V_i + \sum_{1\le i<j\le n} V_{ij} + \ldots + V_{12\ldots n}, \quad (3)$$

where V_i is the portion of the QoI variance associated with the subfunction g_i,

$$V_i = V(g_i(x_i)) = V[\mathbb{E}(y|x_i)], \quad (4)$$

and V_{ij} is the portion of the QoI variance associated with the subfunction g_{ij},

$$V_{ij} = V(g_{ij}(x_i, x_j)) = V[\mathbb{E}(y|x_i, x_j)] - V[\mathbb{E}(y|x_i)] - V[\mathbb{E}(y|x_j)]. \quad (5)$$

Similar expressions can be built up for V_{ijk} and further. Dividing by the total variance, the decomposition of sensitivity indices is obtained,

$$\sum_i S_i + \sum_{1\le i<j\le n} S_{ij} + \ldots + S_{12\ldots n} = 1, \quad (6)$$

where $S_i = V_i/V$, $S_{ij} = V_{ij}/V$, and so on for the higher-order terms. The main effect sensitivity index S_i represents the normalized expected reduction in total variance if the variance of the ith input variable were reduced to zero. Computing these sensitivity indices is termed a global sensitivity analysis (GSA).[44]

III. Uncertainty Budgets in System Design

Figure 2 illustrates our overall uncertainty quantification method. Section III.A describes the initial problem setup. Section III.B formulates a multi-objective optimization problem to solve the resource allocation problem and Section III.C discusses the solution to the optimization problem.

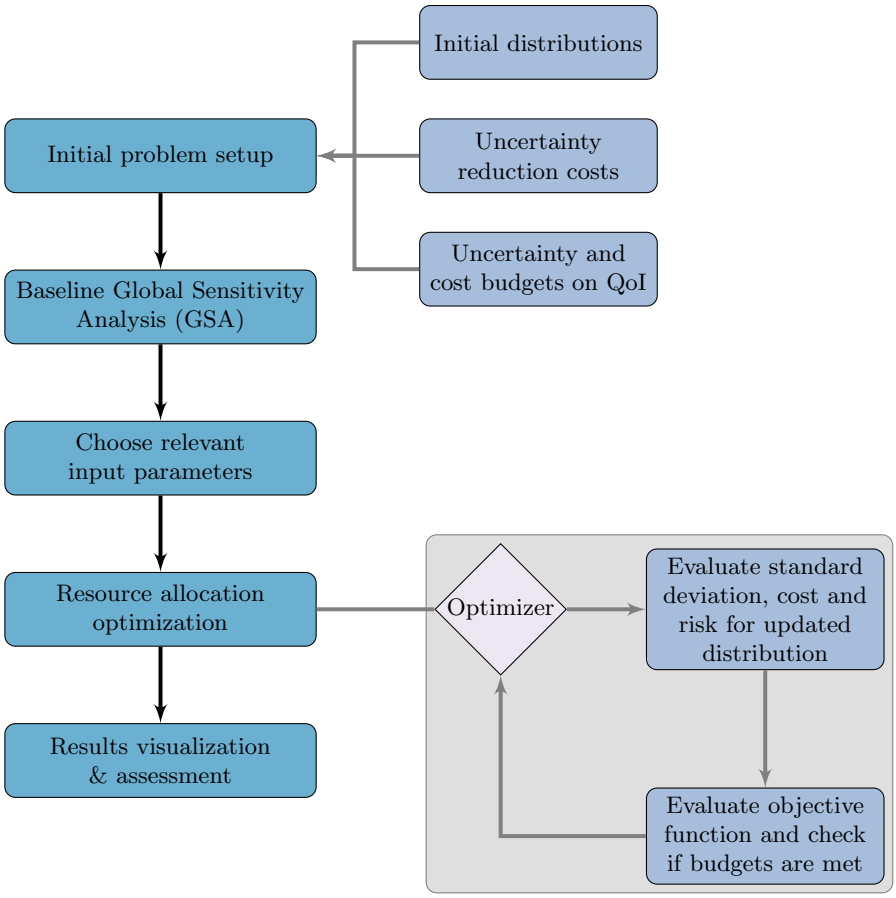

Figure 2. Flow chart showing the uncertainty budgeting methodology.

III.A. Initial problem setup

As shown in Figure 2, the inputs to our methodology are the initial distributions describing uncertainty in each of the system inputs, a model of the costs of uncertainty reduction activities, and cost and uncertainty budgets. The initial uncertainty distribution for each input variable can be constructed from expert elicitation and/or historical data. In this paper, only uniform distributions are considered; therefore in our setting, for each input variable the designer has two degrees of freedom: the mean of the input variable and the standard deviation of the input variable. Thus, with n input variables, the problem has a total of $2n$ degrees of freedom in changing the input variable distributions. Figure 3 illustrates the degrees of freedom in changing a single uniform input distribution. The extension to other distribution types is straightforward, although the resulting parametrization of changes in uncertainty may have more degrees of freedom per input variable.

For the QoI, three budgets are considered: a budget on risk, P_b, a budget on standard deviation, $\sigma_{Y,b}$, and a budget on the cost of changing the input variables' distributions, C_b. Here we use as a risk metric the probability that the QoI fails to meet a requirement, so that the risk budget constraint becomes $\mathbb{P}\left(y > y_{\text{crit}}\right) \leq P_b$, where $\mathbb{P}$ denotes probability, y_{crit} is a critical value that the QoI must not exceed, and P_b is the designer-specified budget on the allowable risk probability. We note that common definitions of risk typically include both the probability of occurrence and the impact of the event, through measures such as semi-deviations, Value at Risk, or Conditional Value at Risk (see, e.g., Ref. 46)—any of these risk measures could be used to define the risk budget. In the formulation presented here, the budgets P_b, $\sigma_{Y,b}$, and C_b are set to be constant, and so there are no correlations among them; however, a straightforward and interesting extension would be to introduce some correlations (e.g., through dependence on a common parameter or through a total budget constraint) and to explore the tradeoffs between allocating budget to cost versus uncertainty.

We also require the specification of a model for the cost of changing the distribution of each input variable.

We consider both the cost of changing the mean input value (i.e., a change in the nominal design with no accompanying change in uncertainty) and the cost of reducing the input variable's uncertainty (i.e., changing the range of the uniform distribution). A change in input variable mean could, for instance, imply a redesign to a less aggressive design in order to reduce variance in the QoI and thus improve design robustness, or a redesign to a higher-performing design in order to decrease risk of not meeting system requirements. The costs of these changes should include the actual redesign activities as well as any costs that might be incurred to advance technologies that underly the new design point. Reducing uncertainty of an input variable would typically be achieved by additional research and development effort, and/or by experiments, again with associated costs.

Given these initial distributions, a baseline GSA estimates the contributions of each uncertain input to the QoI variance as described in Section II.B. The GSA results can then be used to screen for the input parameters with the highest influence on the QoI. If a parameter has a low total sensitivity index, then its effect on QoI variance will be small and it is better to exclude that parameter from the optimization. This will speed up the optimization by reducing the number of degrees of freedom, and will also remove low-sensitivity (flat) regions in the design space that would otherwise hamper the optimization convergence.

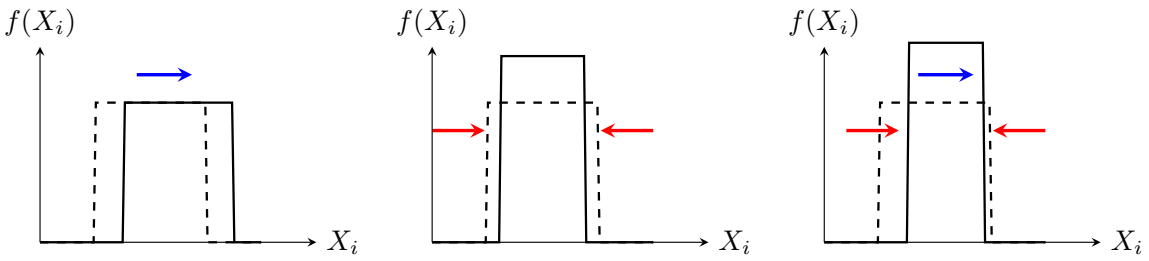

(a) Shift in mean

(b) Reduction in uncertainty

(c) Shift in mean together with a reduction in uncertainty

Figure 3. Illustration of design freedom in changing the parameters of a uniform distribution.

III.B. Resource allocation optimization formulation

Our methodology next formulates the optimal resource allocation strategy as a constrained optimization problem, where the optimization degrees of freedom are the parameters describing the input variable PDFs (in our case, the mean and standard deviation for each input variable). The optimal resource allocation must meet the budgets on cost and uncertainty. It is likely that there are multiple feasible input PDFs that meet those constraints. Our approach is to identify an optimal strategy by forming an objective function that expresses designer preferences on cost, standard deviation and risk. This optimization problem is written as

$$\begin{aligned} \underset{\boldsymbol{\mu},\boldsymbol{\sigma}}{\text{minimize}} \quad & \mathcal{F}(\boldsymbol{\mu},\boldsymbol{\sigma}) &&= \alpha\frac{P(\boldsymbol{\mu},\boldsymbol{\sigma})}{P_b} + \beta\frac{\sigma_Y(\boldsymbol{\mu},\boldsymbol{\sigma})}{\sigma_{Y,b}} + \gamma\frac{C(\boldsymbol{\mu},\boldsymbol{\sigma})}{C_b} \\ \text{subject to} \quad & \mathcal{G}_P(\boldsymbol{\mu},\boldsymbol{\sigma}) &&= P(\boldsymbol{\mu},\boldsymbol{\sigma}) - P_b \leq 0 \\ & \mathcal{G}_\sigma(\boldsymbol{\mu},\boldsymbol{\sigma}) &&= \sigma_Y(\boldsymbol{\mu},\boldsymbol{\sigma}) - \sigma_{Y,b} \leq 0 \\ & \mathcal{G}_C(\boldsymbol{\mu},\boldsymbol{\sigma}) &&= C(\boldsymbol{\mu},\boldsymbol{\sigma}) - C_b \leq 0 \end{aligned} \tag{7}$$

where the designer selects the weighting factors α, β and γ assigned to the risk, standard deviation, and cost, respectively. Here C is the cost associated with changing the input distributions, P is the risk (probability of failing to meet a design requirement), and σ_Y is the standard deviation of the QoI. Each of these three quantities is shown as a function of $\boldsymbol{\mu}$, the vector containing the means of the n input distributions, and $\boldsymbol{\sigma}$, the vector containing the standard deviations of the n input distributions. The terms in the objective function are normalized by the cost, risk and standard deviation budgets, C_b, P_b and $\sigma_{Y,b}$, respectively.

III.C. Solving the resource allocation optimization

Figure 4 depicts the process of solving the optimization problem. Given updated input variable distributions specified by $\boldsymbol{\mu}$ and $\boldsymbol{\sigma}$, we must estimate the QoI standard deviation, risk and cost to evaluate the objective function $\mathcal{F}(\boldsymbol{\mu},\boldsymbol{\sigma})$ and constraints $\mathcal{G}_P(\boldsymbol{\mu},\boldsymbol{\sigma})$, $\mathcal{G}_\sigma(\boldsymbol{\mu},\boldsymbol{\sigma})$, $\mathcal{G}_C(\boldsymbol{\mu},\boldsymbol{\sigma})$.

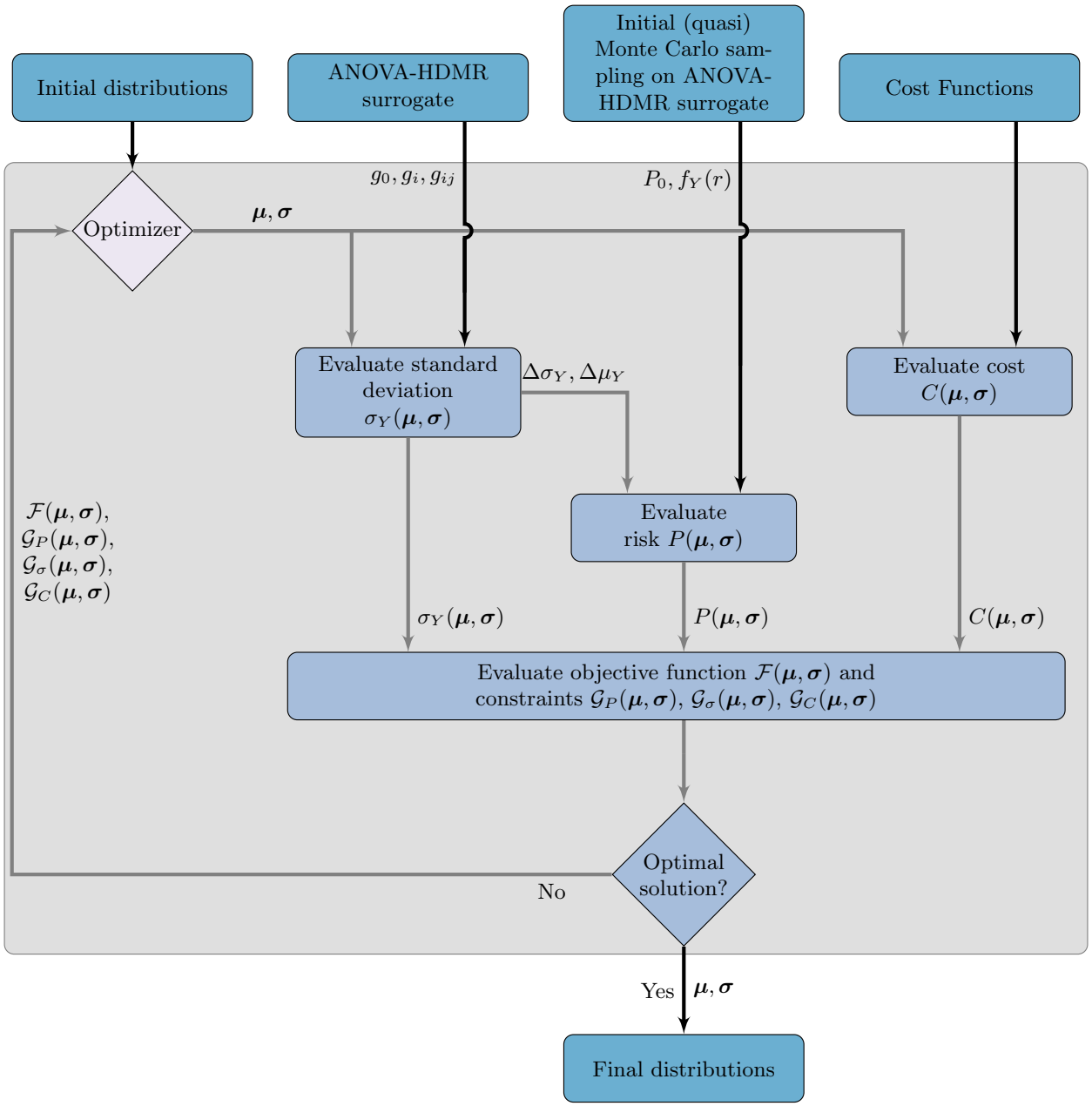

Figure 4. Flow chart for the resource allocation optimization.

In order to solve the optimization problem, the updated standard deviation and risk must be estimated for changes in the input distribution (as provided by the optimizer). For the standard deviation, this requires estimating

$$\sigma_Y'^{\,2} = \int \left(g\left(\mathbf{x}\right) - g_0'\right)^2 f_{\mathbf{x}}'\left(\mathbf{x}\right) \mathrm{d}\mathbf{x} \tag{8}$$

$$\text{where} \quad g_0' = \int g\left(\mathbf{x}\right) f_{\mathbf{x}}'\left(\mathbf{x}\right) \mathrm{d}\mathbf{x}, \tag{9}$$

where $f_{\mathbf{x}}'\left(\mathbf{x}\right)$ is the updated joint probability distribution for the inputs $\mathbf{x}$ and $\sigma_Y'^{\,2}$ is the corresponding updated QoI variance. These integrals can be evaluated using quadrature methods. The risk can be estimated

via Monte Carlo simulation on the updated distribution, using the unbiased estimator $\hat{p}$:

$$P\left(Y > r\right) \approx \hat{p} = \frac{1}{N_s} \sum_{i=1}^{N_s} \mathbb{I}\left(Y_i\right), \tag{10}$$

$$\text{with } \mathbb{I}\left(Y_i\right) = \begin{cases} 1, & \text{if} \quad Y_i > r \\ 0, & \text{if} \quad Y_i \leq r \end{cases}$$

where N_s is the total number of Monte Carlo samples, and $\mathbb{I}\left(Y_i\right)$ is the indicator function.

The uncertainty budgeting methodology presented in this section applies to general models—it requires only the ability to query the model output for specified input values. However, the sampling required to evaluate the QoI standard deviation and risk over many potential input distributions will in general require many model evaluations; that is, solving the optimization problem (7) may be expensive. A primary source of cost is in computing, at each optimization iteration, the integrals that define the expected values, standard deviation and probability of failure. If, for example, one uses standard tensor product quadrature with N_q quadrature points in each dimension, then this would require evaluating the black-box system model $\left(N_q\right)^n$ times, where n is the number of input variables. Although these computations can easily be parallelized, for $n > 3$ one would need to use a more advanced (sparse) quadrature scheme in order to keep the computational costs manageable. A second source of cost is in computing the gradients required at each optimization iteration. Using a finite difference approximation for the gradient requires $2n(N_q)^n$ additional function evaluations in the tensor product quadrature case, since each integral is recomputed for each of the $2n$ optimization variables.

To alleviate the computational cost of these model evaluations, one may use a surrogate model to estimate the objective functions and constraints. While any surrogate model could be used, as described in the next section, HDMR and local sensitivity analysis permit derivation of surrogate models that are tailored to the task at hand. In addition, one of the attractive features of the HDMR surrogate presented in the next section is that the gradient can be derived analytically and computed by evaluating the integrals only along the faces of the hypercube. For example, for a uniform distribution, this reduces the number of function evaluations to compute the gradients to be $2n(N_q)^{(n-1)}$. For more detail on an efficient strategy to compute the gradients, see Ref. 47.

IV. Surrogate Modeling

This section presents a surrogate modeling approach that can be used to reduce the computational expense of solving the uncertainty budgeting optimization problem. Section IV.A describes a surrogate model based on HDMR, used to estimate the updated standard deviation. Section IV.B describes a local approximation that provides a surrogate risk estimate.

IV.A. HDMR-based surrogate

For many systems, it is the case that main (single-variable) effects and two-way interactions dominate the input–output relationship. In such cases, third-order and higher-order terms in the HDMR can be neglected without incurring a large error, permitting an accurate surrogate to be derived via truncation of the HDMR.[37,38] This leads to the approximation

$$\tilde{g}\left(\mathbf{x}\right) \approx g_0 + \sum_{j=1}^{n} g_i\left(x_i\right) + \sum_{1 \leq i < j \leq n} g_{ij}\left(x_i, x_j\right). \tag{11}$$

Following Ref. 43, one can then build a surrogate model by representing the component functions using expansions of an appropriate set of basis functions:

$$g_i\left(x_i\right) \approx \sum_{r=1}^{\ell} \alpha_r^i \varphi_r\left(x_i\right), \tag{12}$$

$$g_{ij}\left(x_i, x_j\right) \approx \sum_{p=1}^{\ell} \sum_{q=1}^{\ell} \beta_{pq}^{ij} \varphi_{pq}\left(x_i, x_j\right), \tag{13}$$

where g_i is represented by ℓ basis functions $\varphi_1, \ldots, \varphi_\ell$, and α_r^i is the coefficient corresponding to the rth basis function. Similarly, g_{ij} is represented by the basis functions φ_{pq} with corresponding coefficients β_{pq}^{ij}. In this work, we use $\varphi_{pq}(x_i, x_j) = \varphi_p(x_i)\,\varphi_q(x_j)$ and we use the same number of basis functions, ℓ, for all input variables, but this need not be the case. We employ orthonormal polynomials as basis functions, so that the coefficients defining the surrogate model are found as[40]

$$\alpha_r^i = \int_{K^n} g(\mathbf{x})\,\varphi_r(x_i)\,f_{\mathbf{x}}(\mathbf{x})\,\mathrm{d}\mathbf{x} \qquad \forall\, r \quad \in \{1, \ldots, \ell\}, \tag{14}$$

$$\beta_{pq}^{ij} = \int_{K^n} g(\mathbf{x})\,\varphi_p(x_i)\,\varphi_q(x_j)\,f_{\mathbf{x}}(\mathbf{x})\,\mathrm{d}\mathbf{x} \quad \forall\, \{p, q\} \in \{1, \ldots, \ell\}. \tag{15}$$

Here K^n is the n-dimensional unit hypercube with $K^n = \{(x_1, x_2, \ldots, x_n) \mid 0 \leq x_i \leq 1\}$.

To construct the HDMR-based surrogate model requires finding all α_r^i and β_{pq}^{ij} by evaluating the integrals in Equations (14) and (15). We evaluate these integrals using Gauss-Legendre quadrature. For a low number of inputs (e.g., less than five) and a relatively smooth response, the behavior of the QoI can typically be characterized over the input space using on the order of tens or hundreds of samples. However, as the number of inputs increases, one would most likely be better off using (quasi) Monte Carlo sampling to resolve the integrals, as in the RS-HDMR method.[43,48] Regardless of the method of integration, the same set of samples can be re-used to find all α_r^i and β_{pq}^{ij}. For instance, if Gauss-Legendre quadrature is used, the function $g(\mathbf{x})$ is evaluated $(N_q)^n$ times, with N_q being the number of quadrature points in each dimension. We then use that set of samples to evaluate each α_r^i and each β_{pq}^{ij}. We choose basis functions that are appropriate for the specified input PDFs; for example, for uniform distributions, we employ shifted Legendre polynomials on the domain $[0, 1]$.

IV.B. Local sensitivity surrogate for risk estimation

For the risk estimation, one can use the HDMR-based surrogate derived in Section IV.A; however, performing Monte Carlo sampling for every change in the input distributions may still be expensive, especially if the risk budget is a small probability value (since estimating a low probability to within acceptable error typically requires many more Monte Carlo samples than estimating the standard deviation). In order to obtain the risk of the QoI more efficiently, one can additionally employ local sensitivity estimates for risk as in Ref. 34. Firstly, we evaluate the risk for the baseline input distributions *once* using Monte Carlo sampling on the surrogate model, and we evaluate the surrogate risk estimator $\hat{p}$ defined in (10), where note now that the QoI y is estimated using the surrogate model rather than the original model g. We denote this baseline risk estimate by P_0. Local sensitivity estimates then provide an approximation for the change in risk due to a change in the mean of the QoI, $\Delta\mu_Y$, as

$$\Delta P_\mu \approx -\Delta\mu_Y\, f_Y(r), \tag{16}$$

and for the change in risk due to a change in the standard deviation of the QoI, $\Delta\sigma_Y$, as

$$\Delta P_\sigma \approx \frac{\Delta\sigma_Y}{\sigma_Y}\,(\mu_Y - r)\,f_Y(r). \tag{17}$$

The risk associated with the updated distribution, P', can then be found cheaply using the approximation

$$P' = P_0 - \Delta\mu_Y\, f_Y(r) + \frac{\Delta\sigma_Y}{\sigma_Y}\,(\mu_Y - r)\,f_Y(r). \tag{18}$$

This local approximation will become inaccurate for large changes in mean or standard deviation. In particular, for certain combinations of parameters, using Eq. (18) can result in negative risk. In that case, we either set the risk to zero or we invoke a full Monte Carlo estimation of the risk.

Using the surrogate models presented in this section introduces errors into the estimation of the standard deviation and risk, and consequently into the solution of the optimization problem. The described surrogate strategies are based on assumptions that have been empirically validated for a wide range of problems in the literature, but for a general model, the magnitude of these modeling errors will be unknown. It is important to note, however, that the surrogate models are used to accelerate the optimization process, but after running the optimization, all solutions of interest are evaluated *a posteriori* using the full model. In this way, we

leverage the surrogate models to make the approach computationally tractable (avoiding repeated Monte Carlo simulations inside the optimization loop) and to find potentially interesting areas of the decision space, but we evaluate and investigate potential uncertainty reduction options using our highest fidelity models. Nonetheless, it is important to note that using the surrogate model may result in suboptimal solutions, since the surrogate model may miss a few potentially optimal decision areas in the space of input variables.

V. Results

The uncertainty budgeting method is applied to an illustrative example that considers conceptual design of a commercial jetliner. The example aircraft is sized using the Transport Aircraft Sizing and OPTimization tool (TASOPT). TASOPT comprises low-order physics-based aircraft sizing models with minimal reliance on empirical and historical data, which makes it appropriate to simulate the changes in design QoIs with respect to changes in input variables.[49] The example problem considers a baseline aircraft based on the Boeing 737-800. We consider a sizing mission with a range of 2950 nautical miles, 180 passengers, and a cruise altitude of 35,000 ft. The first example considers just two uncertain input parameters, so that we can extensively visualize the design space and optimization results; we then consider a more challenging example with six uncertain parameters.

V.A. Problem setup: Propulsion system uncertainty

Our first illustrative example considers the effects of uncertainty in engine technologies on early conceptual aircraft design decisions. The aircraft Maximum Take-off Weight ($MTOW$) is used as the QoI y; this is a quantity that represents many aspects of the overall vehicle design. The uncertainties in propulsion technology are represented by taking the uncertain input variables to be $\mathbf{x} = [T_{\text{metal}}, (T_{t4})_{\text{CR}}]^\top$, where T_{metal} is the maximum allowable temperature of the metal in the turbine blades, and $(T_{t4})_{\text{CR}}$ is the total temperature at the inlet of the turbine at cruise conditions. $(T_{t4})_{\text{CR}}$ is directly related to the thermal efficiency of the engine and is at the same time restricted by T_{metal}. Therefore, it is expected that uncertainty in these two variables will have a large influence on the fuel efficiency and thereby the maximum takeoff weight of the aircraft. It is also expected that there is an interaction between the two variables.

The corresponding distributions for T_{metal} and $(T_{t4})_{\text{CR}}$ are estimated using a combination of information from Federal Aviation Administration (FAA) databases and expert elicitation from FAA consultants.[50] T_{metal} and $(T_{t4})_{\text{CR}}$ are modeled as uniform random variables such that $T_{\text{metal}} \sim U[1172, 1272]$ K and $(T_{t4})_{\text{CR}} \sim U[1541.5, 1641.5]$ K. The initial mean value of T_{metal} is therefore 1222 K with a standard deviation of 28.87 K, and the initial mean of $(T_{t4})_{\text{CR}}$ is 1591.5 K with a standard deviation of 28.87 K. With two input variables with uniform distributions, there are in total four degrees of freedom in changing the distributions of the input variables, since both the mean and standard deviation of each parameter can be altered.

Budgets are set on risk, standard deviation and cost. The risk budget is set such that the probability of $MTOW$ exceeding 1.802×10^5 lb is at most 4%, while the standard deviation of $MTOW$ is required to be at most 450 lb. The cost of changing the distributions of the input variables must remain below 18 cost units. Thus, the budget constraints are written as

$$\mathbb{P}(MTOW > 1.802 \cdot 10^5 \text{ lb}) \leq 4\% = P_b, \quad \sigma_Y \leq 450 \text{ lb} = \sigma_b, \quad C \leq 18 = C_b. \tag{19}$$

The notional cost model for T_{metal} and $(T_{t4})_{\text{CR}}$ is shown in Figure 5. Note that the x-axis has been normalized by their maximum allowable changes due to the different scales of the two input variables. This cost model is used in the optimization process to quantify the cost of making changes in the input distributions. The cost model for changes in mean is asymmetric, because it requires more effort to increase the mean temperature and thus it is more expensive. For T_{metal}, an increase in mean value would, for instance, require using a new material for the turbine, which would be a major design overhaul and might even require developing a new alloy with better thermal properties. The cost budget of 18 units in this example was selected arbitrarily, but chosen to be consistent with the cost model and the problem's levels of uncertainty. When applying this approach in practice, the cost model and budget would be informed by data about personnel requirements, time, equipment, and other resources required to make these changes to the design. In these cases, the cost models and budgets would most likely be cast in units of actual dollars.

To determine an appropriate number of samples to use in the Monte Carlo simulations, we run a convergence study. Figure 6 shows the estimated mean and standard deviation of the $MTOW$ as a function of

the number of samples in the Monte Carlo run. Each plotted point represents an average computed over ten independent Monte Carlo simulation runs. From the plot, it can be seen that acceptable levels of accuracy are achieved with 5000 samples; this number will be used in the following results.

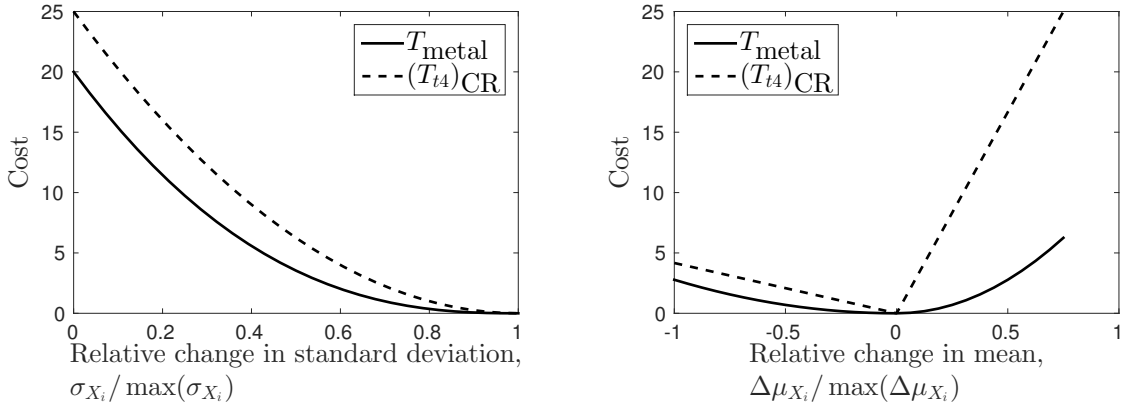

(a) for changes in the input standard deviation

(b) for changes in the input mean

Figure 5. Notional cost model for the two-parameter example.

V.B. Surrogate and sensitivity analysis

We construct an HDMR-based surrogate model using the method described in Section IV. This requires estimating the coefficients α_r^i and β_{pq}^{ij} by evaluating the integrals in Equations (14) and (15). Since the inputs T_{metal} and $(T_{t4})_{\text{CR}}$ are modeled using uniform distributions, we employ shifted Legendre polynomials for the basis functions. The first three shifted Legendre polynomials are

$$\begin{aligned}
\varphi_1(\xi) &= \sqrt{3}\,(2\xi - 1)\,, \\
\varphi_2(\xi) &= 6\sqrt{5}\left(\xi^2 - \xi + \frac{1}{6}\right), \\
\varphi_3(\xi) &= 20\sqrt{7}\left(\xi^3 - \frac{3}{2}\xi^2 + \frac{3}{5}\xi - \frac{1}{20}\right),
\end{aligned} \tag{20}$$

with $0 \le \xi \le 1$. Furthermore, because the number of inputs is low, the integrals in Equations (14) and (15) are solved efficiently using Gauss-Legendre quadrature, requiring a minimum number of TASOPT runs. In this case, only 49 TASOPT runs are required to build the surrogate model.

For purposes of illustration, we assess the convergence of the root mean squared error between the surrogate QoI estimate and the TASOPT QoI estimate for different numbers of quadrature points and orders of basis functions. We use the error definition from Sobol',[42] defined as

$$\begin{aligned}
\delta(g, \tilde{g}) &= \frac{1}{V}\int \left[g(\mathbf{x}) - \tilde{g}(\mathbf{x})\right] \mathrm{d}\mathbf{x} \\
\text{with } V &= \int \left[g(\mathbf{x}) - g_0\right]^2 \mathrm{d}\mathbf{x}.
\end{aligned} \tag{21}$$

Here g is the actual function mapping input to QoI (here the TASOPT simulation), $\tilde{g}$ is the truncated ANOVA-HDMR surrogate model, and V is the variance associated with the actual QoI.

Figure 7 shows the convergence of the error $\delta(g, \tilde{g})$, where we solve the integral in Eq. (21) using quasi Monte Carlo sampling with 5000 samples. For this problem, a choice of $N_q = 7$ quadrature points in each dimension and fifth-order basis functions leads to a surrogate model with acceptably low error (below 10^{-5}). As mentioned above, this surrogate is constructed with just 49 TASOPT evaluations. To further illustrate the accuracy of the surrogate model, TASOPT is evaluated at 225 points in the interior in order to compare estimates of $MTOW$ over the design space. Figure 8 shows the resulting contours of $MTOW$ estimated by TASOPT and by the surrogate model.

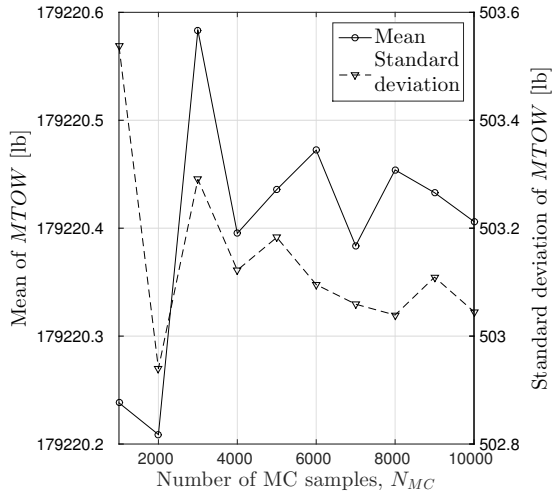

Figure 6. Convergence of the Monte Carlo simulation for different numbers of Monte Carlo samples.

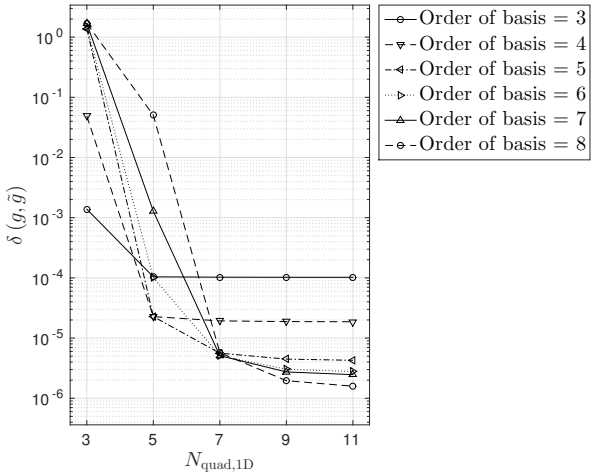

Figure 7. Convergence of $\delta(g, \tilde{g})$ for different numbers of quadrature points and different orders of basis functions.

Figure 9 shows the GSA results using the HDMR-based surrogate model. The results show that T_{metal} accounts for an expected 10% of the *MTOW* variance, while $(T_{t4})_{\text{CR}}$ is responsible for 75%. $(T_{t4})_{\text{CR}}$ is directly related to the fuel efficiency of the engine; it is therefore expected that it contributes a larger portion of the uncertainty in the maximum take-off weight. Lastly, in line with expectations, a considerable interaction term between the two variables accounts for the remaining 15% of the variance in *MTOW*. Both input parameters have considerable influence on the uncertainty in the QoI and therefore both are included in the resource allocation optimization.

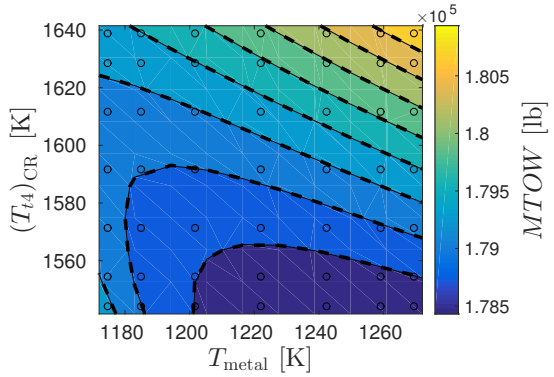

Figure 8. *MTOW* estimated by surrogate model (solid lines) compared to TASOPT (dashed lines). The circles indicate the quadrature points used to create the surrogate model.

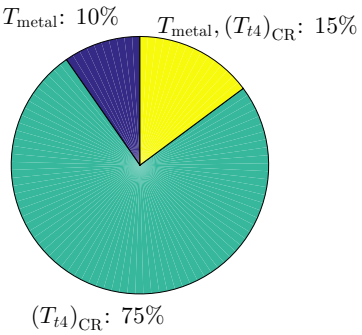

Figure 9. Sensitivity analysis results from the HDMR-based surrogate model.

V.C. Design space visualization

Visualization of the design space can provide the designer with useful insight into the effects on QoI uncertainty and cost of changing the input distribution parameters. We explore the design space via a series of two-dimensional plots, as shown in the pairwise contour plot for risk in Figure 10(a) and for standard deviation in Figure 10(b). These slices are generated by evaluating the risk, cost, and standard deviation of the QoI in the same way as in Figure 4, only now for a specified $\boldsymbol{\mu}$ and $\boldsymbol{\sigma}$. We vary $\boldsymbol{\mu}$ and $\boldsymbol{\sigma}$ to generate

a contour plot. We slice through the design space by varying two design parameters (e.g., the mean and standard deviation of one particular input variable) and fixing the other design parameters at the mean value of their respective nominal distributions. For problems with higher-dimensional inputs, we note that this visualization will be much more challenging, since the two-dimensional plots will represent only a tiny fraction of the overall design space. In higher dimensional cases, more sophisticated visualization techniques will be needed, such as those described in Ref. 51.

The general shape of these contours is consistent with expectations based on knowledge of the design problem: as the input standard deviation is reduced, the risk is reduced because the output distribution is more concentrated around the mean. However, the plots also show a large area where the risk is zero; therefore, it is expected that there are multiple ways to achieve a minimum-risk solution. Furthermore, Figure 10(b) shows that, for this problem, a reduction in input standard deviation has a larger effect on the QoI standard deviation than a shift in input mean.

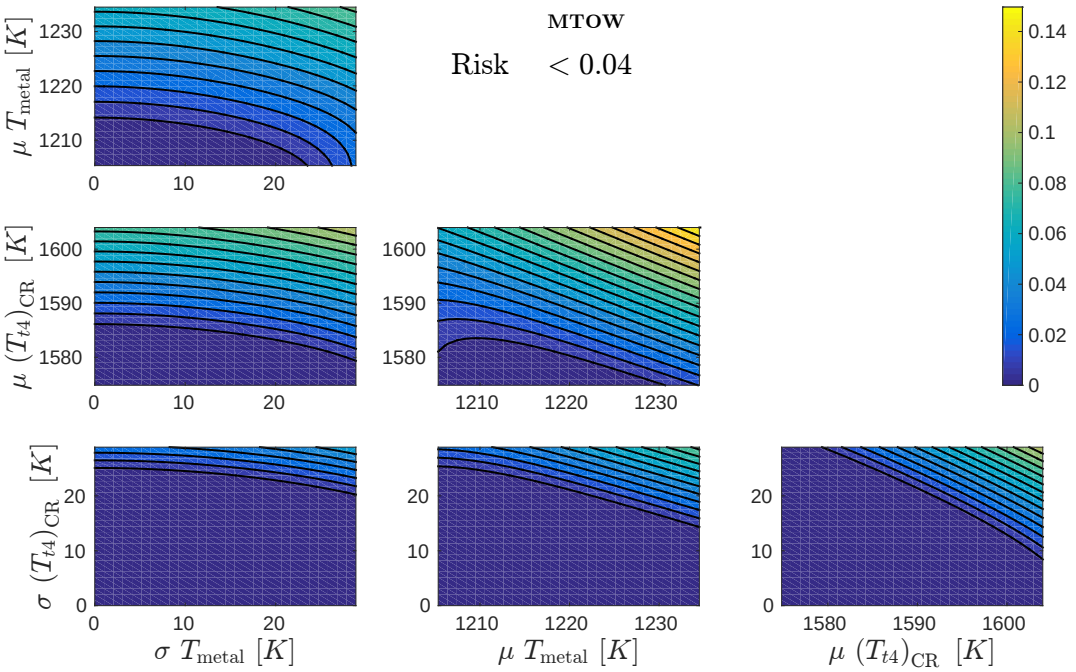

(a) Risk

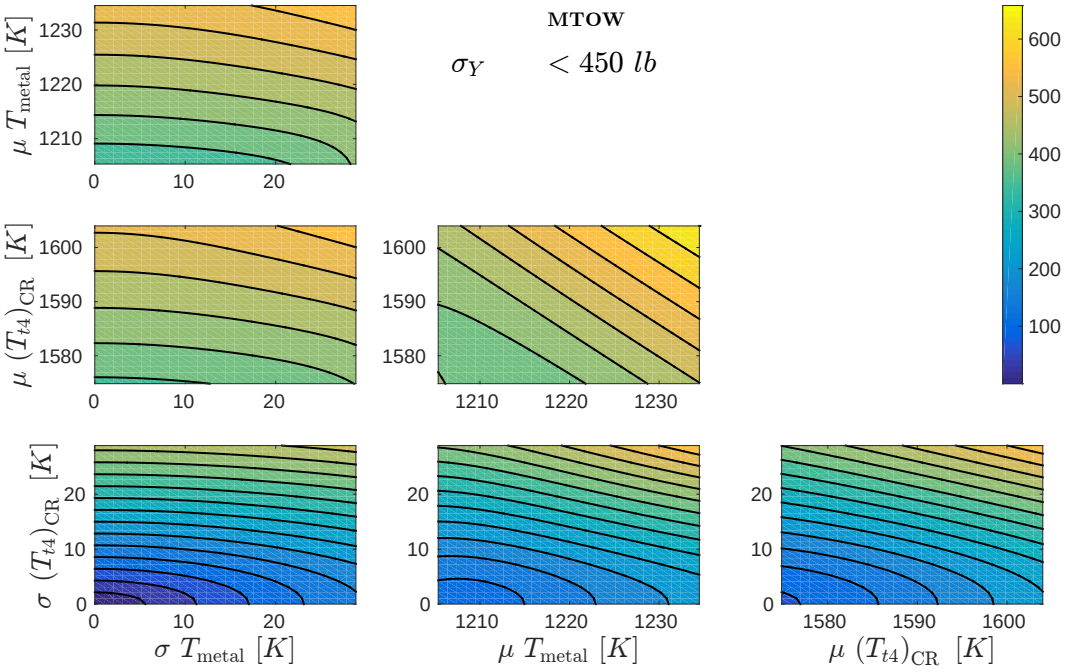

(b) Standard deviation (lb)

Figure 10. Pairwise contour plot of QoI risk and QoI standard deviation as a function of changes in input means and input standard deviations.

Applying the budget constraints to the estimated surfaces of risk, standard deviation and cost defines a feasible region with respect to each budget constraint. Overlaying the results allows for visualizing the feasible

design space, i.e., the range of input distribution changes for which all budget constraints are met. This is shown in Figure 11, where the darkest area indicates the feasible region. Other shaded areas correspond to region where only one or two of the three budget constraints are met. For this problem, it can be seen that the feasible region is mostly constrained by the cost and standard deviation budgets. This is consistent with the previous result that showed a large area of low-risk solutions.

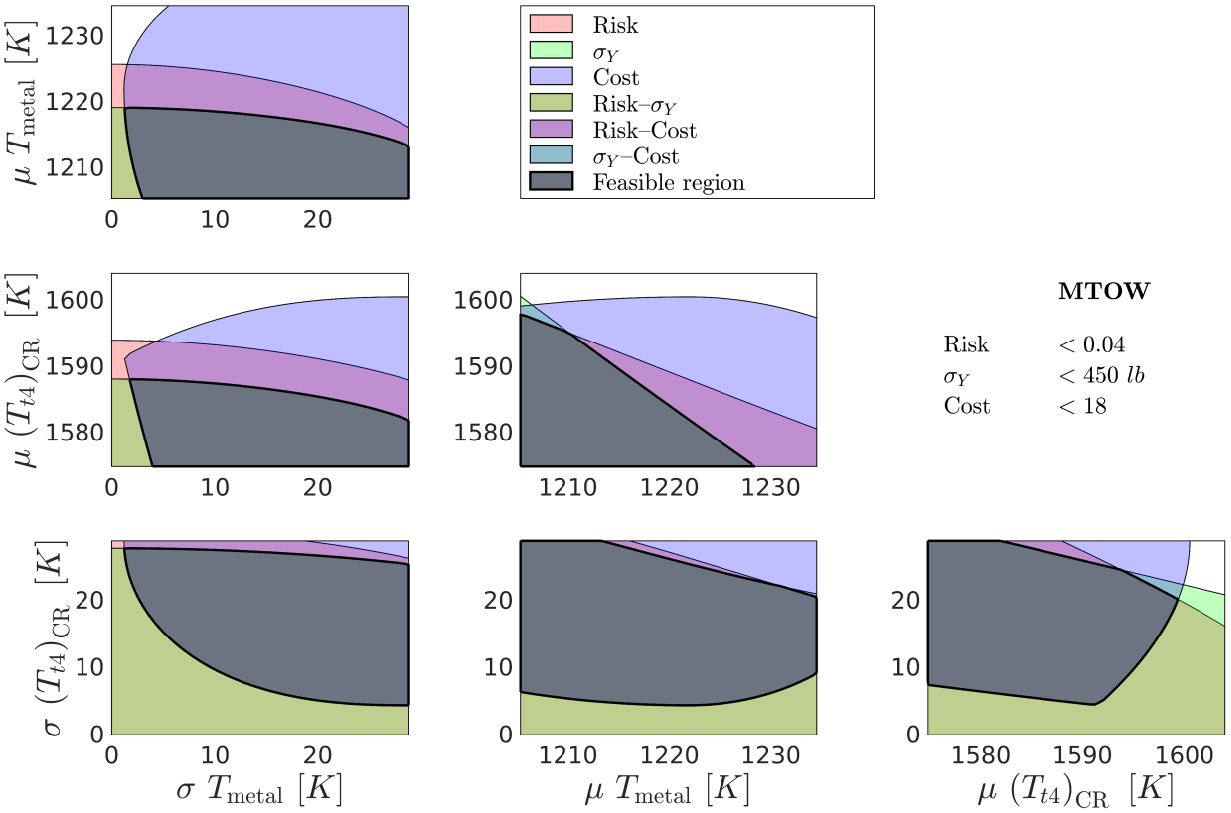

Figure 11. Feasible area in the design space, satisfying risk, standard deviation and cost budgets. Also shown are the areas that satisfy one or two of the three budgets.

V.D. Resource allocation optimization

The initial uncertainty distributions on T_{metal} and $(T_{t4})_{\text{CR}}$ lead to the distribution of $MTOW$ shown in Figure 12. The corresponding initial estimate of standard deviation is $\sigma_Y = 503.13$ lb and of risk is $\hat{p} = 5.49\%$. Both the standard deviation and the risk exceed the specified uncertainty budgets. We now solve the optimization problem (7) to determine redesign options that will reduce uncertainty to below the specified levels, while also satisfying the allowable cost budget. We solve the optimization problem using the Method of Moving Asymptotes[52] within `NLopt`[b].[53] Because the design space is non-convex, we run each optimization from several different initial conditions. While this helps to avoid being trapped in a local minimum, it does not guarantee that we find a globally optimal solution.

[b] `NLopt` is a nonlinear optimization library by Steven G. Johnson, available at `http://ab-initio.mit.edu/wiki/index.php/NLopt`.

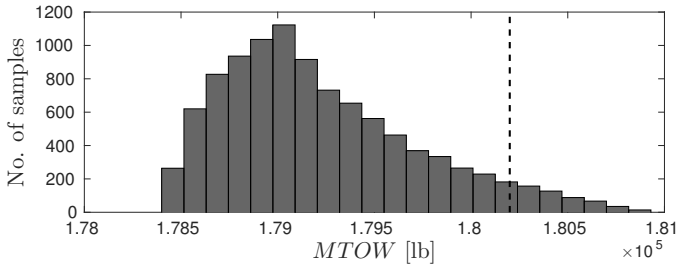

Figure 12. Histogram of *MTOW* using 10,000 quasi Monte Carlo samples (dashed line indicates the not-exceed-value for risk).

Figures 13(a) and 13(b) show optimal solutions for two cases: minimum standard deviation ($\alpha = \gamma = 0,\ \beta = 1$), and equal weighting among risk, standard deviation and cost ($\alpha = \beta = \gamma = 1$). The radar plots indicate the relative changes in mean values and standard deviations from the baseline initial values for each design variable. Figure 13(a) indicates that relatively large changes to the original input distributions are required to achieve the minimum-standard-deviation solution. This solution is achieved by a 32% standard deviation reduction for T_{metal} while shifting its mean to 1210 K, and a standard deviation reduction of 74% for $(T_{t4})_{\text{CR}}$ while shifting its mean to 1584 K. This results in 0% risk, a QoI standard deviation of 109 lb, and an associated cost of 18 cost units. In this case, the active cost constraint is preventing further reductions in QoI standard deviation. In this solution, the required standard deviation reduction for $(T_{t4})_{\text{CR}}$ is larger than for T_{metal}, which is consistent with the GSA results in Figure 9, although the cost models play an important role in determining the optimal uncertainty reduction balance across inputs.

The optimal solution for equal weighting among risk, standard deviation, and cost (Figure 13(b)) shows less dramatic changes in the input distributions than the solution for minimum standard deviation. For this problem, this result is due to cost now playing a role in the objective function. We can see, for instance, that the mean of $(T_{t4})_{\text{CR}}$ is barely changed, because it is expensive to do so (see Figure 5). The equally-weighted optimal solution is achieved by a standard deviation reduction of 15% for T_{metal} with its mean shifting to 1212 K, and a standard deviation reduction of 32% for $(T_{t4})_{\text{CR}}$ with its mean unaltered. These changes result in 0% risk, a QoI standard deviation of 306 lb, and an associated cost of 3.6 cost units.

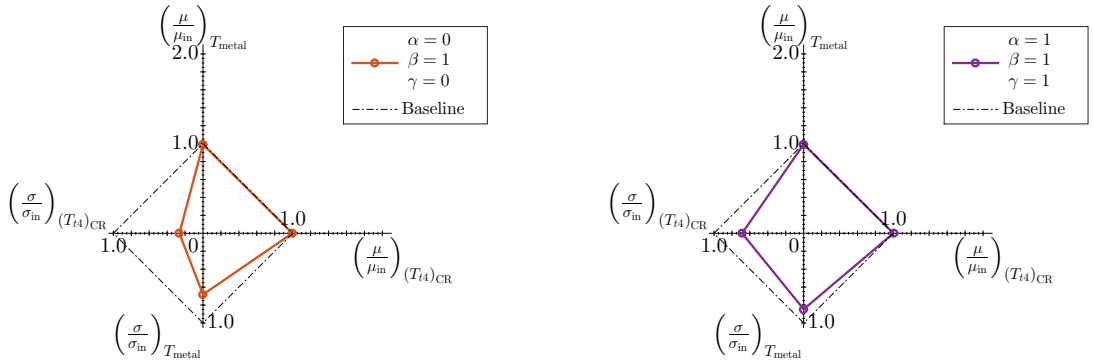

(a) Minimum standard deviation

(b) Equally important

Figure 13. Optimum resource allocation strategy for two different objective functions. Left: minimum standard deviation ($\alpha = \gamma = 0,\ \beta = 1$). Right: equal weighting among risk, standard deviation and cost ($\alpha = \beta = \gamma = 1$). Scales: 0 K $< \mu_{T_{\text{metal}}} <$ 2444 K, 0 K $< \mu_{(T_{t4})_{\text{CR}}} <$ 3183 K, 0 K $< \sigma_{T_{\text{metal}}} <$ 28.87 K, 0 K $< \sigma_{(T_{t4})_{\text{CR}}} <$ 28.87 K.

Instead of looking at an individual optimization result for a single combination of α, β and γ, a Pareto front gives the designer more insight into the tradespace of uncertainty reduction options. We generate a Pareto front by running the optimization for different values of α, β and γ. In Figure 14, the Pareto front is projected onto the cost–standard deviation plane for *MTOW*, with the radar plots depicting the corresponding solution values for the optimization variables for three different points. The minimum-cost solution is that for which there are almost no changes in the input distribution and for which the requirements

are just barely met (i.e., the standard deviation is exactly 450 lb and the risk is close to 4%). This minimum-cost solution requires only a small standard deviation reduction in T_{metal} of 6% while shifting its mean to 1219.4 K, and a standard deviation reduction in $(T_{t4})_{\text{CR}}$ of 7% with no change in its mean. These updated input distributions then result in a QoI standard deviation of 450 lb with a risk of 3.3% and an associated cost of 0.23 cost units. In contrast, the minimum-standard-deviation solution requires considerable changes in the input distribution and just barely meets the cost budget, as already explained and shown in Figure 13(a).

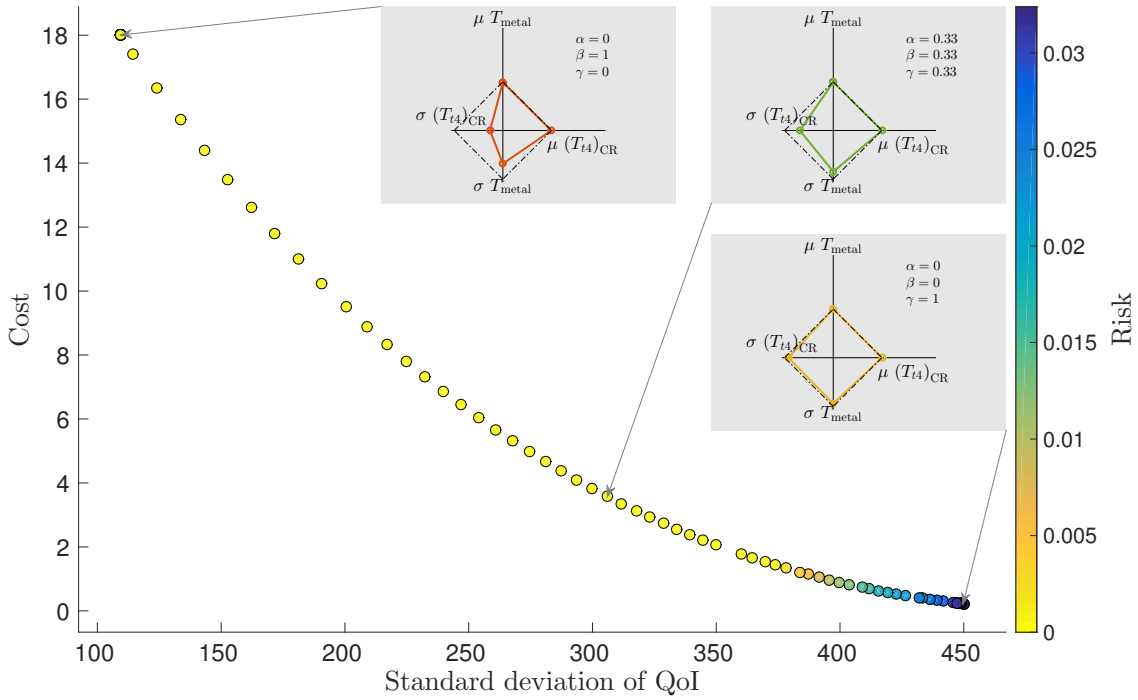

Figure 14. Pareto front projected onto the cost – standard deviation plane of *MTOW*.

Lastly, we plot the changes in distributions for some of the optimal solutions. Figure 15 shows the initial and updated input distributions that correspond to the equally-weighted optimized solution. Figure 16 compares the initial QoI PDF and the QoI PDF resulting from the optimal uncertainty reduction choices, for the minimum-cost solution and equally-weighted solution. For the purposes of illustration, the QoI PDFs are estimated using kernel density estimation with 10,000 samples drawn from the surrogate. The vertical line indicates the do-not-exceed-value r, which is used to evaluate the risk of the solutions. Figure 16 shows that the change in QoI distribution for the minimum-cost solution is small, but leads to a sufficient reduction in risk to satisfy the budget constraints. For the equally-weighted solution, the change is more significant; the standard deviation is considerably smaller and the risk approaches zero.

V.E. Assessment of optimization results

A final step in the methodology is to evaluate the most interesting (according to designer preferences) results from the optimization, using the original model in place of the surrogate. In our case, this assessment is performed by evaluating the uncertainty in TASOPT estimates of MTOW, using the updated distributions for T_{metal} and $(T_{t4})_{\text{CR}}$. As an illustration, we execute this process for four different objectives: minimum risk, minimum standard deviation, minimum cost, and equal cost/risk/standard deviation weighting. In each case, we evaluate TASOPT at 5,000 input samples using quasi Monte Carlo sampling, and estimate the variance and risk of the *MTOW* QoI. Table 1 compares the results to those estimated using the surrogate model. The relative errors are all small, indicating that the surrogate modeling approach introduces little error.

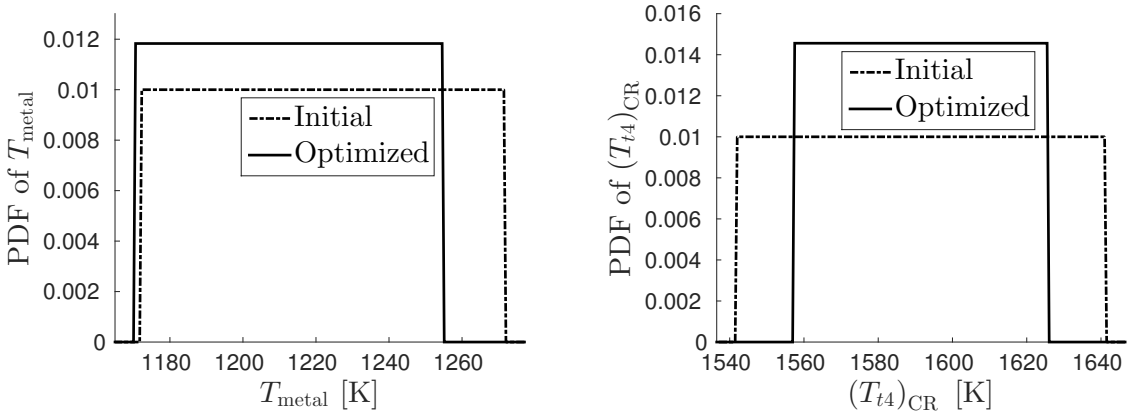

(a) T_{metal} (b) $(T_{t4})_{\text{CR}}$

Figure 15. Initial PDFs for input variables T_{metal} and $(T_{t4})_{\text{CR}}$ compared to updated PDFs for the equally-weighted optimal solution ($\alpha = \beta = \gamma = 1$).

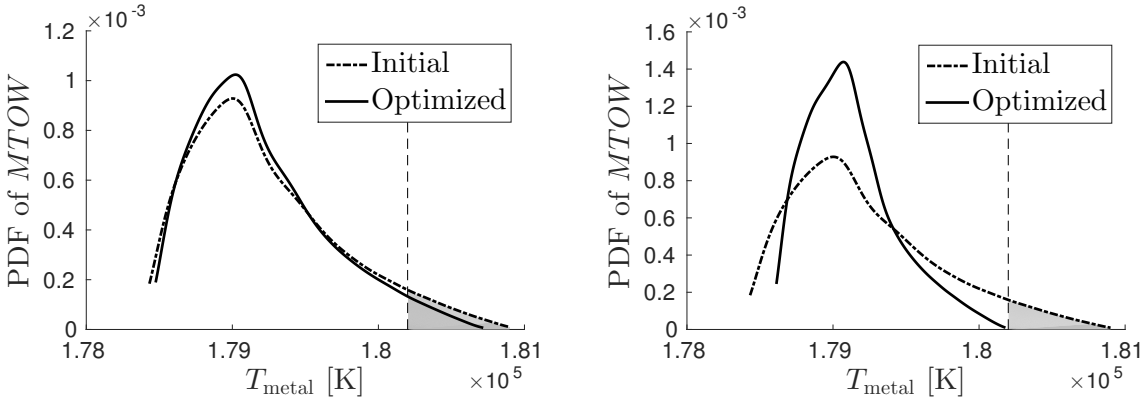

(a) $\alpha = \beta = 0$, $\gamma = 1$ (for minimum cost) (b) $\alpha = \beta = \gamma = 1$ (for all equally important)

Figure 16. Initial *MTOW* QoI PDF compared to updated PDF for two different optimal solutions.

Table 1. Risk and standard deviation estimates of optimal strategies; TASOPT estimates compared to surrogate model estimates.

	Surrogate		TASOPT	
Objective	Risk	σ_Y [lb]	Risk	σ_Y [lb]
Minimum Risk	0	109.5	0	109.5
Minimum σ_Y	0	109.4	0	109.5
Minimum Cost	0.033	449.6	0.033	449.7
Equally important	0	305.7	0	305.6

V.F. Aircraft system uncertainty

We consider now a more complex example that includes a larger number of uncertain parameters drawn from different disciplines across the aircraft system design problem. Propulsion uncertainty is represented by the variables T_{metal}, $(T_{t4})_{CR}$ and OPR, the overall pressure ratio of the engine. Structural uncertainties

are represented by uncertainty in the maximum allowable fuselage shell bending stress, s_{fus}, and in the maximum allowable wing and tail spar cap stress, s_{wt}. The lift coefficient during cruise, C_L, represents an aerodynamic uncertainty. As quantities of interest, we use both $PFEI$ and $MTOW$.

To create the six-dimensional surrogate model is more challenging than in the two-dimensional case, since using a tensor product quadrature rule as before, would require $(N_q)^6$ sampling points. Instead if we neglect the higher-order terms in the HDMR—using the so-called cut-HDMR[38]—the required number of samples reduces to $\binom{6}{2}(N_q)^2$. We build up a surrogate for this six-dimensional input space using $N_q = 7$ quadrature points in each dimension and fifth-order basis functions. This yields an acceptable error with only 735 TASOPT function evaluations.

For the resource allocation problem, we place similar budgets on the design as in Section V.A:

$$\begin{aligned}\mathbb{P}(MTOW > 1.810 \cdot 10^5 \text{ lb}) \leq 5\% = P_{b_1}, \quad \sigma_{Y_1} \leq 600 \text{ lb} = \sigma_{Y,b_1}, \quad C \leq 25 = C_b \\ \mathbb{P}(PFEI > 8.47 \text{ KJ/kg} \cdot \text{km}) \leq 4\% = P_{b_2}, \quad \sigma_{Y_2} \leq 0.16 \text{ KJ/kg} \cdot \text{km} = \sigma_{Y,b_2},\end{aligned}$$

where the subscript 1 corresponds to the MTOW QoI and the subscript 2 refers to the PFEI. However, we relax the budgets slightly because there is more uncertainty in the initial design with respect to the problem in Section V.A and the consideration of two QoIs introduces additional budget constraints. We again use a notional cost model for the parameters, as shown in Figure 17.

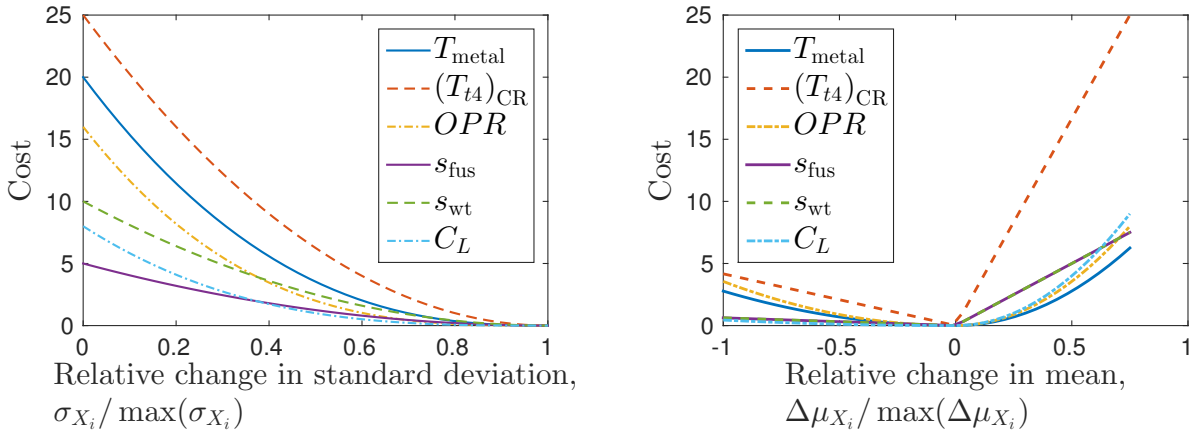

(a) for changes in the input standard deviation

(b) for changes in the input mean

Figure 17. Notional cost model for the six-parameter example.

We now consider multiple QoIs and therefore reformulate Eq. (7) into

$$\begin{aligned}
\underset{\boldsymbol{\mu},\boldsymbol{\sigma}}{\text{minimize}} \quad & \mathcal{F}(\boldsymbol{\mu},\boldsymbol{\sigma}) = \textstyle\sum_{j=1}^{2} \alpha_j \dfrac{P(\boldsymbol{\mu},\boldsymbol{\sigma})}{P_{b_j}} + \sum_{j=1}^{2} \beta_j \dfrac{\sigma_{Y_j}(\boldsymbol{\mu},\boldsymbol{\sigma})}{\sigma_{Y,b_j}} + \gamma \dfrac{C(\boldsymbol{\mu},\boldsymbol{\sigma})}{C_b} \\
\text{subject to} \quad & \mathcal{G}_{P_1}(\boldsymbol{\mu},\boldsymbol{\sigma}) = P_1(\boldsymbol{\mu},\boldsymbol{\sigma}) - P_{b_1} \leq 0 \\
& \mathcal{G}_{P_2}(\boldsymbol{\mu},\boldsymbol{\sigma}) = P_2(\boldsymbol{\mu},\boldsymbol{\sigma}) - P_{b_2} \leq 0 \\
& \mathcal{G}_{\sigma_1}(\boldsymbol{\mu},\boldsymbol{\sigma}) = \sigma_{Y_1}(\boldsymbol{\mu},\boldsymbol{\sigma}) - \sigma_{Y,b_1} \leq 0 \\
& \mathcal{G}_{\sigma_2}(\boldsymbol{\mu},\boldsymbol{\sigma}) = \sigma_{Y_2}(\boldsymbol{\mu},\boldsymbol{\sigma}) - \sigma_{Y,b_2} \leq 0 \\
& \mathcal{G}_{C}(\boldsymbol{\mu},\boldsymbol{\sigma}) = C(\boldsymbol{\mu},\boldsymbol{\sigma}) - C_b \leq 0.
\end{aligned} \tag{22}$$

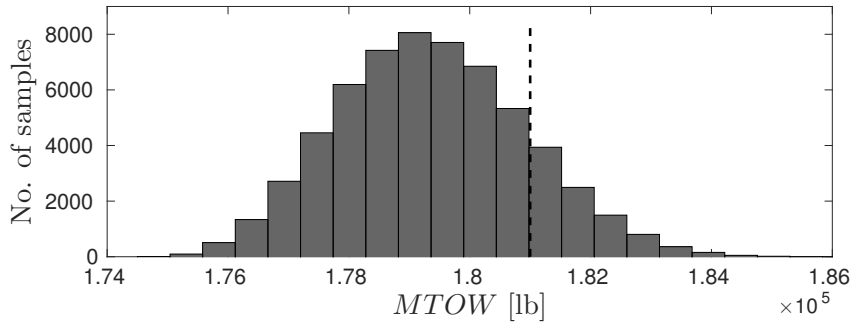

(a) $MTOW$

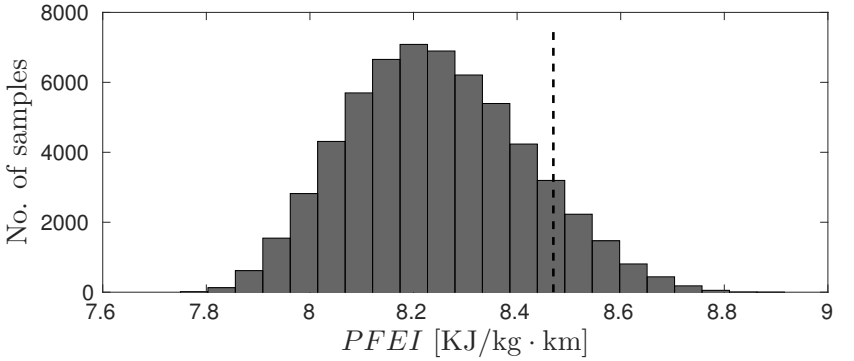

(b) $PFEI$

Figure 18. Histograms of *MTOW* and *PFEI* using 60,000 quasi Monte Carlo samples in the six-parameter example (dashed line indicates the do-not-exceed-value for risk).

For the initial input parameter distributions, the resulting standard deviation of $MTOW$ is estimated to be 1553 lb, while the standard deviation of $PFEI$ is estimated to be 0.172 KJ/kg · km. These initial input parameter distributions lead to a distribution of $MTOW$ and $PFEI$ as in Figure 18. The corresponding initial risk estimate for $MTOW$ is 15% and the risk estimate for $PFEI$ is 11%.

Table 2. Optimal mean and standard deviation for input parameters for six-parameter example.

Parameter	μ	σ
T_{metal} [K]	1212.9	18.3
$(T_{t4})_{CR}$ [K]	1591.5	15.6
OPR [−]	26.24	0.50
s_{fus} [Psi]	3.000e4	135
s_{wt} [Psi]	3.000e4	59.0
C_L [−]	0.5772	1.03e-3

Using these budgets and initial distributions, we perform the resource allocation optimization. Figure 19 presents the results where the objective function is to minimize the sum of the $MTOW$ standard deviation and the $PFEI$ standard deviation. The optimization results for this objective function are listed in Table 2. We see that indeed all budgets are satisfied in Table 2. The general trend shows mostly large uncertainty reductions in the structural parameters (s_{fus} and s_{wt}) and the aerodynamics parameter C_L. There are still uncertainty reductions in the engine parameters, because they have such a large influence on the uncertainty in the QoIs; however, according to our cost model (Figure 17), changes in those engine parameters are costly and are therefore kept to a minimum. This trend is also seen in the minimum-cost solution, where the changes in the engine parameters are kept to a minimum.

Again, given our optimized input distributions we assess the accuracy of the approximations used during the optimization problem solution. Therefore, we rerun the original model in place of the surrogate model, with the optimized input distributions. This assessment is performed by running a quasi Monte Carlo

Table 3. Comparison of estimated risk, standard deviation, and expected values between the HDMR surrogate and a Monte Carlo simulation with 15,000 TASOPT samples for the six-parameter example. In both cases the cost budget constraint is active at $C = 25.0$.

Parameter	HDMR	MC
Risk $MTOW$	0%	0%
Risk $PFEI$	0%	0%
σ_Y $MTOW$ [lb]	398	398
σ_Y $PFEI$ $\left[\frac{\text{KJ}}{\text{kg}\cdot\text{km}}\right]$	0.089	0.088
$\mathbb{E}[MTOW]$ [lb]	1.791e5	1.791e5
$\mathbb{E}[PFEI]$ $\left[\frac{\text{KJ}}{\text{kg}\cdot\text{km}}\right]$	8.203	8.202

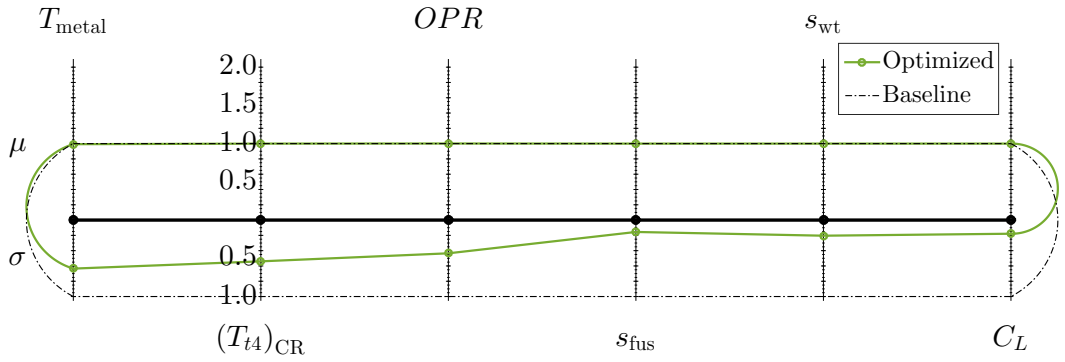

Figure 19. Results for the six-parameter example resource allocation optimization for minimum combined standard deviation ($\beta_1 = \beta_2 = 1$, $\alpha_1 = \alpha_2 = \gamma = 0$).

simulation with 15,000 samples of TASOPT, from which we then compute the variance and risk of the QoIs. Those results are shown in Table 3, labeled by "MC". The results from the optimization using the original ANOVA-HDMR expansion and the local sensitivity estimates are labeled "HDMR". We see that both the standard deviation and the risk agree well.

The results from this multidisciplinary problem illustrate how our uncertainty budgeting methodology can help guide designers on where to reduce uncertainty and where to target design changes. This is turn allows decision-makers to identify early in the design process where they need to allocate more resources to meet requirements. For the illustrative example presented here, a decision could be, for instance, to focus efforts towards uncertainty reduction in the structural and aerodynamic components of the design. The new input distributions would serve as quantifiable targets for the uncertainty of the structures and aerodynamics design groups. We also note that this process of managing uncertainty is an iterative process—at each stage of the design process, different levels of uncertainty and risk can be tolerated and this will translate into evolving targets across the disciplinary design groups.

VI. Conclusion

This paper presents an uncertainty budgeting approach for supporting conceptual design decisions, and illustrates the approach on an example problem. An HDMR-based surrogate model allows for fast and accurate estimates of the QoI standard deviation and risk, evaluated as a function of changes in the distributions of uncertain inputs. The tradespace of re-design and uncertainty reduction decisions can then be evaluated and visualized; a multi-objective optimization problem can also be solved to determine a specific resource allocation strategy that balances cost and uncertainty reduction. This supports designers in deciding which areas require additional resources for maximum benefit. While the probabilistic analysis presented here may be somewhat costly to conduct, the decisions it is intended to support involve the allocation of significant resources (money, time, facilities and people).

The first illustrative example considers the influence of uncertainties in propulsion technology on the

overall conceptual design of a commercial aircraft. The results highlight the kinds of useful conclusions that may be drawn from the analysis. In the case considered, the uncertainties in engine technology are represented by T_{metal}—the maximum allowable temperature of the metal in the turbine—and $(T_{t4})_{\text{CR}}$—the total temperature at the inlet of the turbine. For the specific analysis case studied, $(T_{t4})_{\text{CR}}$ has the largest influence on the uncertainty in the Maximum Take-off Weight ($MTOW$) of the aircraft, while the interaction between T_{metal} and $(T_{t4})_{\text{CR}}$ is also responsible for a substantial part of the uncertainty in $MTOW$. The resource allocation optimization leads to solutions for which the standard deviation of $(T_{t4})_{\text{CR}}$ is reduced more than the standard deviation of T_{metal}, reflecting this higher sensitivity. A second example considers the influence of system-wide uncertainties—in propulsion technology, material properties, and aerodynamic performance parameters—on the overall conceptual aircraft design. The resource allocation optimization shows that for the specific problem analyzed, the best strategy is to "spend" the uncertainty budget by targeting a large uncertainty reduction in the material properties and the aerodynamic performance, and only a small uncertainty reduction in the propulsion technology. This result would permit a design group to assign quantitative re-design targets to each disciplinary sub-group.

In both cases, the optimization yields strategies for which the changes in mean value are much smaller (relatively speaking) than the changes in input standard deviation. While the solutions found here reflect our particular problem set up and our chosen notional cost model, which places a large penalty on changes in the mean design point, this general result is consistent with many conceptual design problems where the cost of design changes are large. This paper aims not to recommend a specific aircraft design choice, but rather to provide a general methodology by which the designer can systematically explore these tradeoffs between design modifications and uncertainty reduction. We note that the bulk of multidisciplinary design optimization methods focus on finding a single "optimal design"—even if uncertainty is included, the problem is still usually formulated as finding a single optimal design that minimizes some statistic of the QoI. However, the analysis enabled by our methodology suggests that focusing on uncertainty reduction rather than just design changes may be a more productive approach. A potential area of future work is to integrate the uncertainty budgeting methodology with a multi-level design formulation, such as ATC. This would enable consideration of more complex systems, as well as greater insight into the role of cascading uncertainties between subsystem levels. Another area of future work is to develop more sophisticated budget models, such as those that include correlation between cost and uncertainty budgets, and to use sensitivity results from the optimization solution to determine the relative gains of increasing or decreasing budget limits.

Acknowledgements

This work was supported in part by the NASA LEARN program through grant number NNX14AC73A, technical monitor Justin S. Gray, and by the United States Department of Energy Applied Mathematics Program, Awards DE-FG02-08ER2585 and DE-SC0009297, program manager Steven Lee, as part of the DiaMonD Multifaceted Mathematics Integrated Capability Center.

References

[1]Haldar, A. and Mahadevan, S., *Probability, Reliability and Statistical Methods in Engineering Design*, John Wiley & Sons, Inc., New York, NY, 2000.

[2]Roy, C. J. and Oberkampf, W. L., "A Comprehensive Framework for Verification, Validation, and Uncertainty Quantification in Scientific Computing," *Computer Methods in Applied Mechanics and Engineering*, Vol. 200, 2011, pp. 2131–2144.

[3]Mavris, D. N., Bandte, O., and DeLaurentis, D. A., "Robust Design Simulation: A Probabilistic Approach to Multidisciplinary Design," *Journal of Aircraft*, Vol. 36, No. 1, 1999, pp. 298–307.

[4]Smith, R., *Uncertainty Quantification: Theory, Implementation, and Applications*, SIAM, Philadelphia, 2014.

[5]Oberkampf, W. L., DeLand, S. M., Rutherford, B. M., Diegert, K. V., and Alvin, K. F., "Error and Uncertainty in Modeling and Simulation," *Reliability Engineering and System Safety*, Vol. 75, 2002, pp. 333–357.

[6]Ang, A. H.-S. and Tang, W. H., *Probability Concepts in Engineering: Emphasis on Applications to Civil and Environmental Engineering*, John Wiley & Sons, Inc., Hoboken, NJ, 2nd ed., 2007.

[7]Kennedy, M. C. and O'Hagan, A., "Bayesian Calibration of Computer Models," *Journal of the Royal Statistical Society, Series B*, Vol. 63, No. 3, 2001, pp. 425–464.

[8]Cacuci, D., Ionescu-Bujor, M., and Navon, I., *Sensitivity And Uncertainty Analysis: Applications to Large-Scale Systems (Volume II)*, Chapman & Hall, 2005.

[9]Helton, J. C., Johnson, J. D., Sallaberry, C. J., and Storlie, C. B., "Survey of Sampling-Based Methods for Uncertainty and Sensitivity Analysis," *Reliability Engineering and System Safety*, Vol. 91, 2006, pp. 1175–1209.

[10]Aughenbaugh, J. M. and Paredis, C. J., "The Value of Using Imprecise Probabilities in Engineering Design," *Journal of Mechanical Design*, Vol. 128, No. 4, 2006, pp. 969–979.

[11]Venter, G., Haftka, R. T., and Starnes, J. H., "Construction of Response Surface Approximations for Design Optimization," *AIAA Journal*, Vol. 36, No. 12, 1998, pp. 2242–2249.

[12]Eldred, M. S., Giunta, A. A., and Collis, S. S., "Second-Order Corrections for Surrogate-Based Optimization with Model Hierarchies," *10th AIAA/ISSMO Multidisciplinary Analysis and Optimization Conference, AIAA Paper 2004-4457*, Albany, NY, 2004.

[13]Simpson, T. W., Peplinski, J. D., Koch, P. N., and Allen, J. K., "Metamodels for Computer-Based Engineering Design: Survey and Recommendations," *Engineering with Computers*, Vol. 17, No. 2, 2001, pp. 129–150.

[14]Alexandrov, N. M., Lewis, R. M., Gumbert, C. R., Green, L. L., and Newman, P. A., "Approximation and Model Management in Aerodynamic Optimization with Variable-Fidelity Models," *Journal of Aircraft*, Vol. 38, No. 6, 2001, pp. 1093–1101.

[15]Queipo, N. V., Haftka, R. T., Shyy, W., Goel, T., Vaidyanathan, R., and Tucker, P. K., "Surrogate-based Analysis and Optimization," *Progress in Aerospace Sciences*, Vol. 41, No. 1, 2005, pp. 1–28.

[16]Lee, S. H. and Chen, W., "A Comparative Study of Uncertainty Propagation Methods for Black-box-type Problems," *Structural and Multidisciplinary Optimization*, Vol. 37, No. 3, 2009, pp. 239–253.

[17]Saltelli, A., Chan, K., and Scott, E. M., *Sensitivity Analysis*, John Wiley & Sons, Inc., New York, NY, 2000.

[18]Homma, T. and Saltelli, A., "Importance Measures in Global Sensitivity Analysis of Nonlinear Models," *Reliability Engineering & System Safety*, Vol. 52, No. 1, 1996, pp. 1–17.

[19]Sobol', I. M., "Sensitivity Estimates for Nonlinear Mathematical Models," *Mathematical Modeling and Computational Experiment*, Vol. 1, No. 4, 1993, pp. 407–414.

[20]Sobol', I. M., "Theorems and Examples on High Dimensional Model Representation," *Reliability Engineering & System Safety*, Vol. 79, No. 2, 2003, pp. 187–193.

[21]Chan, K., Saltelli, A., and Tarantola, S., "Sensitivity Analysis of Model Output: Variance-Based Methods Make the Difference," Proceedings of the 1997 Winter Simulation Conference, 1997.

[22]Saltelli, A. and Bolado, R., "An Alternative Way to Compute Fourier Amplitude Sensitivity Test (FAST)," *Computational Statistics and Data Analysis*, Vol. 26, 1998, pp. 445–460.

[23]Liu, H., Chen, W., and Sudjianto, A., "Relative Entropy Based Method for Probabilistic Sensitivity Analysis in Engineering Design," *Journal of Mechanical Design*, Vol. 128, No. 2, 2006, pp. 326–336.

[24]Knoll, F. and Vogel, T., *Design for Robustness*, IABSE (International Association for Bridge and Structural Engineering), Zurich, Switzerland, 2009.

[25]Taguchi, G., *The System of Experimental Design: Engineering Methods to Optimize Quality and Minimize Costs (2 vols.)*, UNIPUB/Kraus International Publications and American Supplier Institute, White Plains, NY and Dearborn, MI, 1987.

[26]Phadke, M. S., *Quality Engineering Using Robust Design*, Prentice Hall, Englewood Cliffs, NJ, 1989.

[27]Chen, W., Allen, J. K., Tsui, K.-L., and Mistree, F., "Procedure for Robust Design: Minimizing Variations caused by Noise Factors and Control Factors," *Journal of Mechanical Design*, Vol. 118, No. 4, 1996, pp. 478–485.

[28]Du, X., Sudjianto, A., and Chen, W., "An integrated framework for optimization under uncertainty using inverse reliability strategy," *Journal of Mechanical Design*, Vol. 126, No. 4, 2004, pp. 562–570.

[29]Kim, H. M., Michelena, N. F., Papalambros, P. Y., and Jiang, T., "Target Cascading in Optimal System Design," *Journal of Mechanical Design*, Vol. 125, No. 3, 2003, pp. 474–480.

[30]Kokkolaras, M., Mourelatos, Z. P., and Papalambros, P. Y., "Design optimization of hierarchically decomposed multilevel systems under uncertainty," *Journal of mechanical design*, Vol. 128, No. 2, 2006, pp. 503–508.

[31]Kokkolaras, M., "Reliability Allocation in Probabilistic Design Optimization of Decomposed Systems using Analytical Target Cascading," *12th AIAA/ISSMO Multidisciplinary Analysis and Optimization Conference, Victoria, British Columbia, Canada, Paper No. AIAA-2008-6040*, September 10–12 2008.

[32]Chen, X., Molina-Cristóbal, A., Guenov, M., Datta, V. C., and Riaz, A., "A Novel Method for Inverse Uncertainty Propagation," *EUROGEN 2015*, Glasgow, UK, September 14–16 2015.

[33]Padulo, M., Campobasso, M. S., and Guenov, M. D., "Novel uncertainty propagation method for robust aerodynamic design," *AIAA journal*, Vol. 49, No. 3, 2011, pp. 530–543.

[34]Curran, C. and Willcox, K., "Sensitivity Analysis Methods for Mitigating Uncertainty in Engineering System Design," *56th AIAA/ASCE/AHS/ASC Structures, Structural Dynamics, and Materials Conference, Kissimee, FL, Paper No. AIAA-2015-0899*, January 5–9 2015.

[35]He, Q., *Uncertainty and Sensitivity Analysis Methods for Improving Design Robustness and Reliability*, Ph.D. thesis, Massachusetts Institute of Technology, June 2014.

[36]Torenbeek, E., *Synthesis of subsonic airplane design : an introduction to the preliminary design, of subsonic general aviation and transport aircraft, with emphasis on layout, aerodynamic design, propulsion, and performance*, Delft University Press Nijhoff Sold and distributed in the U.S. and Canada by Kluwer Boston, Delft The Hague Hingham, MA, 1982.

[37]Rabitz, H., Aliş, Ö. F., Shorter, J., and Shim, K., "Efficient input-output model representations," *Computer Physics Communications*, Vol. 117, No. 1, 1999, pp. 11–20.

[38]Rabitz, H. and Aliş, Ö. F., "General foundations of high-dimensional model representations," *Journal of Mathematical Chemistry*, Vol. 25, No. 2-3, 1999, pp. 197–233.

[39]Alış, Ö. F. and Rabitz, H., "Efficient implementation of high dimensional model representations," *Journal of Mathematical Chemistry*, Vol. 29, No. 2, 2001, pp. 127–142.

[40]Wang, S.-W., Georgopoulos, P. G., Li, G., and Rabitz, H., "Random sampling-high dimensional model representation (RS-HDMR) with nonuniformly distributed variables: application to an integrated multimedia/multipathway exposure and dose model for trichloroethylene," *The Journal of Physical Chemistry A*, Vol. 107, No. 23, 2003, pp. 4707–4716.

[41]Li, G. and Rabitz, H., "General formulation of HDMR component functions with independent and correlated variables," *Journal of Mathematical Chemistry*, Vol. 50, No. 1, 2012, pp. 99–130.

[42]Sobol, I. M., "Theorems and examples on high dimensional model representation," *Reliability Engineering & System Safety*, Vol. 79, No. 2, 2003, pp. 187–193.

[43]Li, G., Wang, S.-W., and Rabitz, H., "Practical approaches to construct RS-HDMR component functions," *The Journal of Physical Chemistry A*, Vol. 106, No. 37, 2002, pp. 8721–8733.

[44]Saltelli, A., *Global sensitivity analysis : the primer*, John Wiley, Chichester, England Hoboken, NJ, 2008.

[45]Sobol, I. M., "Global sensitivity indices for nonlinear mathematical models and their Monte Carlo estimates," *Mathematics and computers in simulation*, Vol. 55, No. 1-3, 2001, pp. 271–280.

[46]Shapiro, A., Dentcheva, D., and Ruszczyński, A., *Lectures on stochastic programming. Modeling and theory*, Vol. 9 of *MPS/SIAM Series on Optimization*, Society for Industrial and Applied Mathematics (SIAM), Philadelphia, PA; Mathematical Programming Society (MPS), Philadelphia, PA, 2nd ed., 2014.

[47]Opgenoord, M. M. J., *Uncertainty Budgeting Methods for Conceptual Aircraft Design*, SM thesis, Massachusetts Institute of Technology, Cambridge, MA, February 2016.

[48]Li, G., Hu, J., Wang, S.-W., Georgopoulos, P. G., Schoendorf, J., and Rabitz, H., "Random sampling-high dimensional model representation (RS-HDMR) and orthogonality of its different order component functions," *The Journal of Physical Chemistry A*, Vol. 110, No. 7, 2006, pp. 2474–2485.

[49]Drela, M., "N3 Aircraft Concept Designs and Trade Studies – Appendix," Tech. Rep. NASA CR-2010-216794/VOL2, 2010.

[50]Amaral, S., *A Decomposition-Based approach to Uncertainty Quantification of Multicomponent Systems*, Ph.D. thesis, Massachusetts Institute of Technology, June 2015.

[51]Kanukolanu, D., Lewis, K., and Winer, E., "A multidimensional visualization interface to aid in trade-off decisions during the solution of coupled subsystems under uncertainty," *Journal of Computing and Information Science in Engineering*, Vol. 6, No. 3, 2006, pp. 288–299.

[52]Svanberg, K., "A class of globally convergent optimization methods based on conservative convex separable approximations," *SIAM journal on optimization*, Vol. 12, No. 2, 2002, pp. 555–573.

[53]Johnson, S. G., "The NLopt nonlinear-optimization package," http://ab-initio.mit.edu/nlopt.